THE CONSTRUCTION OF DEMONSTRATION LABORATORY KIT FOR MEASURING THE MAGNETIC FIELD BY SMARTPHONE APPLICATION: A CASE OF STRAIGHT ELECTRICAL WIRE

PATHOM VONGVIZAY

Graduate School Srinakharinwirot University

2024

การสร้างชุดทดลองสาธิตเพื่อการวัดสนามแม่เหล็กโดยใช้แอพพลิเคชันของสมาร์ทโฟน: กรณีสายไฟตรง

Pathom VONGVIZAY

ปริญญานิพนธ์นี้เป็นส่วนหนึ่งของการศึกษาตามหลักสูตร
การศึกษามหาบัณฑิต สาขาวิชาฟิสิกส์
คณะวิทยาศาสตร์ มหาวิทยาลัยศรีนครินทรวิโรฒ
ปีการศึกษา 2567

THE CONSTRUCTION OF DEMONSTRATION LABORATORY KIT FOR MEASURING THE MAGNETIC FIELD BY SMARTPHONE APPLICATION: A CASE OF STRAIGHT ELECTRICAL WIRE

PATHOM VONGVIZAY

A Thesis Submitted in Partial Fulfillment of the Requirements

for the Degree of MASTER OF EDUCATION

(Physics)

Faculty of Science, Srinakharinwirot University

2024

THE THESIS TITLED

THE CONSTRUCTION OF DEMONSTRATION LABORATORY KIT FOR MEASURING THE MAGNETIC FIELD BY SMARTPHONE APPLICATION: A CASE OF STRAIGHT ELECTRICAL WIRE

BY

PATHOM VONGVIZAY

HAS BEEN APPROVED BY THE GRADUATE SCHOOL IN PARTIAL FULFILLMENT OF THE REQUIREMENTS FOR THE MASTER OF EDUCATION IN PHYSICS AT SRINAKHARINWIROT UNIVERSITY

(Assoc. Prof. Dr. Chatchai Ekpanyaskul, MD.)

Dean of Graduate School

ORAL DEFENSE COMMITTEE

.... Major-advisor	.... Chair
(Assoc. Prof. Dr.Pongkaew Udomsamuthirun)	(Asst. Prof. Dr.Arpapong Changjan)
.... Co-advisor	.... Committee
(Dr.Suppanyou Meakniti)	(Asst. Prof. Dr.Siriluk Ruangrungrote)

Title	THE CONSTRUCTION OF DEMONSTRATION LABORATORY KIT FOR MEASURING THE MAGNETIC FIELD BY SMARTPHONE APPLICATION: A CASE OF STRAIGHT ELECTRICAL WIRE
Author	PATHOM VONGVIZAY
Degree	MASTER OF EDUCATION
Academic Year	2024
Thesis Advisor	Assoc. Prof. Dr. Pongkaew Udomsamuthirun
Co Advisor	Dr. Suppanyou Meakniti

This study aimed to develop a demonstration laboratory kit for studying magnetic fields based on Ampere's Law and to evaluate its effectiveness. The research was divided into two parts: measuring the magnetic field of a current-carrying straight wire and assessing AC current in electrical equipment. In the first part, magnetic fields were recorded at multiple distances across five circuit configurations, with resistors arranged in series and parallel. Measurements were conducted from 1 cm to 8 cm on both sides of the wire, with the calculated magnetic permeability deviating by less than 10% from standard values, confirming high accuracy. In the second part, magnetic fields were measured at close distances (1 cm and 2 cm from the wire) in circuits connected to an electrical appliance across four configurations, yielding consistent results. The average current ranged from 0.370 A to 1.730 A, with multimeter and clamp meter readings showing percentage errors between 1.42% and 5.83%, indicating satisfactory consistency. These findings affirm the kit's potential as an accessible prototype for physics laboratories.

Keyword : Ampere's Law, Demonstration laboratory kit, Magnetic field, magnetic permeability, Phyphox

ACKNOWLEDGEMENTS

The researcher would like to express deep appreciation to the Thailand International Cooperation Agency (TICA), Ministry of Foreign Affairs of Thailand, for generously providing scholarships throughout the course duration and for supporting this research.

Special thanks go to Assoc. Prof. Dr. Pongkaew Udomsamuthirun, my thesis advisor, for offering invaluable guidance on all research challenges, assisting in the completion of this thesis, and inspiring me to see it through to the end. I am deeply grateful for this opportunity.

I would like to extend my heartfelt gratitude to Asst. Prof. Dr. Arpapong Changjan for his kindness and support in chairing the oral examination of my thesis. His guidance and expertise have been invaluable throughout this process.

Heartfelt appreciation to Asst. Prof. Dr. Siriluk Ruangrungrote, Chairman of the Curriculum Executive Committee, Master's Program in Physics at Srinakharinwirot University, for invaluable knowledge, encouragement, and support through challenges.

I thank Dr. Suppanyou Meakniti, my co-advisor, and Dr. Grittichon Chanilkul for their essential guidance, ensuring a smooth research process. I am also grateful to Mr. Tunyanop Nilkamjon and staff for their assistance with equipment and tool advice crucial to this research.

Finally, I would like to extend my sincere gratitude to all my friends in the Master's Degree Program in the Physics Department, Faculty of Science, at Srinakharinwirot University. Lastly, I am deeply thankful to my family for their unwavering support throughout this journey.

PATHOM VONGVIZAY

TABLE OF CONTENTS

LIST OF TABLE

LIST OF FIGURES

CHAPTER 1
INTRODUCTION

The study of magnetic phenomena aids in understanding the behavior of magnetic area produced by electric currents, and magnetic theory leads to the creation of useful electrical devices such as generators and electric motors. Consequently, this chapter discusses the historical background and theories of the magnetic field.

1.1 Historical background

The science of knowledge holds significant importance for both humans and a country's development. It fosters human cognitive growth by promoting analytical, layered, and rational thinking (Habermas, 2015). Understanding this science serves as a crucial foundation, enabling individuals to navigate the scientific process with enthusiasm while emphasizing the link between studying, researching, and creating knowledge. Therefore, everyone should strive to develop competency in knowledge science to effectively apply relevant knowledge to current situations. This approach aligns logically with 21^{st} century learning principles that stress essential skills like literacy, numeracy, problem-solving, communication, collaboration, creativity and perpetuating uninterrupted knowledge advancement (Guo & Woulfin, 2016).

Based on the concepts and explanations provided, the researcher, as the educational leader, grasp fundamental physics and aim to enhance students' knowledge and comprehension. Understanding the concept of magnetic fields in science necessitates a creative approach. To enhance technicians' understanding and explore the phenomena in detail, constructing an abstract mental image is imperative, as it relies on real-world phenomena to form concepts. While experimental results aided explanations, most apparatuses used to demonstrate magnetic field phenomena were costly and only showcased the effects. Unfortunately, students couldn't conduct experiments due to insufficient equipment at the school. Interviews with students revealed that comprehending this content posed challenges, leading to difficulties in test performance (Cucos & Iucu, 2020). To reinforce accurate scientific concepts, students conducted experiments through simple, low-cost tasks using smartphone media, facilitating rapid acquisition of new information (Setiawan, Septianto, Suhendra, & Iskandar, 2017). To leverage cost-effective learning methods, the researcher designed a series of experimental tasks easily executed with smartphones for study magnetic force fields. Employing investigative learning in collaborative groups served as their learning management system. This approach, categorized as active learning, aimed to prompt students to develop skills through active participation, fostering idea generation, collective thinking, and action, and seeking scientific information, prioritizing students' creation of their knowledge. Through teaching a little, students managed to learn substantially, nurturing positive attitudes toward science learning and lifelong learning skills (Daggol, 2017).

Physics, a critical branch of science, delves into various natural phenomena, demanding imaginative thinking, research, and reasoning to elucidate physical causes and effects (Chamonwang & Chanunun, 2023). Regarded as the cornerstone of science, physics finds extensive applications in daily life, underpinning most technological advancements (Galili, 2018). It serves as the bedrock for both theoretical and applied knowledge. However, the prevailing low performance in physics education suggests that many students grapple with understanding it due to its abstract nature, which necessitates imaginative comprehension (Thipwan, Somprasong, Nattiphon, Rattanasuda, & Thanaphong, 2021). Consequently, schools must prioritize the development of learning management strategies to bolster students' grasp of physics. Studying physics is indispensable, and learning activities should complement theoretical knowledge by fostering active participation, direct experience through experimentation, and problem-solving within groups (Thipwan et al., 2021). Encouraging students to independently summarize experiment results and draw connections between different concepts is paramount. One method to enhance understanding involves creating simple alternating current magnetic field measuring devices for teaching and learning, prioritizing hands-on experience, and reinforcing basic knowledge through skill development, experimentation, and practical applications.

Integrating technology into physics education can elevate student engagement and accessibility, leveraging the omnipresence of smartphones in modern life as valuable learning tools (Thipwan et al., 2021).Recognizing this, the researcher devised a series of demonstration laboratory kit to study Ampere's Law using a straight wire, coupled with an application to record magnetic field intensity at each stage. These activities aimed to facilitate and to make comprehension easier for students, including observing magnetic field formation both before and during the release of electric current into the wire. Additionally, tests were employed to gauge students' attainment in learning about Ampere's Law using a straight wire.

In a significant experiment, Faraday discovered that the value of a conductor changes when magnetic flux passes through a coil. The electromotive force (emf) resulting from this phenomenon is illustrated in Figure 1. Induction occurs in the coil, where the direction of the induced emf opposes that of the original emf (Halliday, Resnick, & Jearl, 2007).

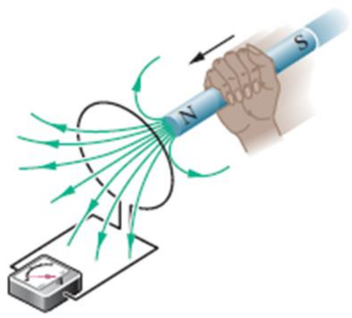

Figure 1 The electric current generated by the moving magnetic coil is detected by an ammeter.

Source: (Halliday et al., 2007)

For a general surface, the total magnetic flux passes the surface is the integral surface of the field lines when the surface area is divided into infinitesimal components.

$$\Phi_B = \int \vec{B} \bullet d\vec{A} \tag{1-1}$$

When Φ_B is the magnetic flux field

$\vec{B}$ is the magnetic field

$d\vec{A}$ is the differential area vector on the surface pass which the magnetic zone passes

The magnetic area through the coil resulted from the relative motion between the wire and magnet. As the magnetic flux through the coil changed over time, an induced emf (ε) was generated. In the coil, the induced emf was a rate of change of magnetic flux field per unit of time, as described by the equation.

$$\varepsilon = -N \frac{d\Phi_B}{dt} \qquad (1\text{-}2)$$

Where ε is the induced emf up in volts (V).

$d\Phi_B$ is the magnetic flux that changes with time dt

N is the number of turns of the coil.

The magnetic field is generated by the electric current flowing through the conductor, as described by Ampere's law, one of the fundamental laws of electromagnetism. According to ampere's circuit law, the current flowing through a closed loop is determined by the integral line of the magnetic field. Ampere's law could be expressed as the line integral of the magnetic field surrounding a closed loop, multiplied by the algebraic sum of the currents flowing through the loop. This formula enables the computation of the magnetic field surrounding a conductor (I) that generates a magnetic field due to current flow (Zangwill, 2013).

$$\oint \vec{B} \bullet d\vec{\ell} = \mu_0 I \qquad (1\text{-}3)$$

Here $d\ell$ is an infinitely small length of the closed path.

μ_0 is the magnetic permeability of vacuum.

I is the current through the element.

The ampere's law can therefore be stated as circulation of the magnetic area along any closed path surrounded I is equal to $\mu_0 I$.

Consider the case of a very long conductor carrying current, influenced by a symmetrically rotating magnetic field. There is a circular path with the conductor at its center, as shown in Figure 2, for a circular magnetic field with a radius defined by the equation (1-4).

$$B = \frac{\mu_0 I}{2\pi a} \tag{1-4}$$

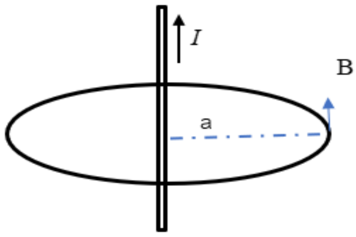

Figure 2 Compasses near a current-carrying wire reveal circular magnetic field lines around it.

Source: (Zangwill, 2013).

The magnetic field, denoted as ($\vec{B}$), delineates the region where a magnet's influence is potent. Within this region, magnetic forces exert their influence on electric charges in motion (Yang, Liu, & Wu, 2023). This field forms a continuous loop, emanating from the north pole (N) and circulating back to the south pole (S). This characteristic allows for the visualization of the magnetic field's orientation by maneuvering a compass around the magnet and noting the deflection of the compass needle, as depicted in Figure 3 (Griffiths, 2023).

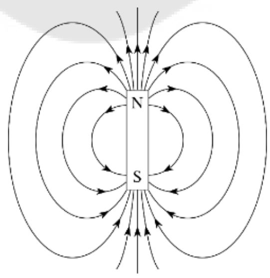

Figure 3 The flux line of magnetic field from magnet.

Source: (Griffiths, 2023)

A permanent magnet is Positioned within a magnetic field, causing the bar magnet to align in the north and south directions according to Earth's magnetic field (Likkason, 2014). The end pointing towards the north is known as the north pole, while the end pointing towards the south is termed the south pole. The Earth could be likened to a magnetic rod, with the south pole corresponding to the north pole in geography and the north pole corresponding to the geographic south pole.

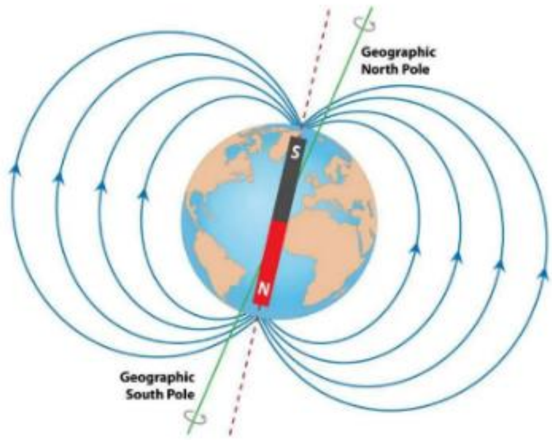

Figure 4 Poles of the earth's magnetic field and geographic poles.

Source: (Likkason, 2014)

According to Biot-Savart's Law the magnetic zone produced by a long straight wire is utilized to determine the magnitude of the magnetic field intensity surrounding a long conductor with a coil of any shape (ℓ), carrying an electric current of (I) amperes, as illustrated in Figure 5. This process involves applying the Biot-Savart law and employing the current-field direction rule: the thumb indicates the direction of the electric current flow (I) within the conductor wire, while the four fingers indicate the direction of the resulting magnetic zone (Drory, 2023).

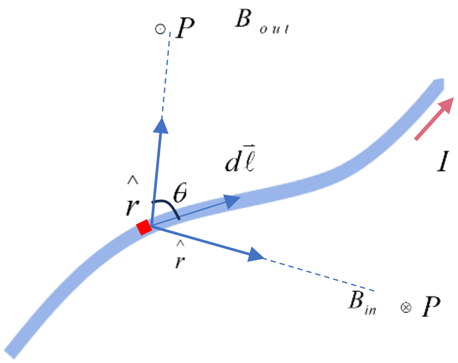

Figure 5 Magnetic field generated by electric current in conductors of any shape.

Source: (Drory, 2023)

Finding the magnitude of the magnetic field strength (B) that is done by dividing the conductor into smaller sections ($d\vec{\ell}$) which is a vector of direction to the current flow (I) cause a small magnetic field ($d\vec{B}$) with the direction of the paper or pointing towards the paper at the point (P) the orientation of the magnetic field depends on the direction of a current flowing in the area of interest, even if it is far from the conductor (r) by giving ($\hat{r}$) was a unit vector representing direction r $\left(\vec{r}=r\hat{r}\right)$ and a small magnetic field ($d\vec{B}$) that was perpendicular to ($d\vec{\ell}$) Therefore, the equation would be as follows:

$$d\vec{B}=\frac{\mu_0}{4\pi}\frac{Id\vec{\ell}\times\vec{r}}{r^3}=\frac{\mu_0}{4\pi}\frac{Id\ell\sin\theta}{r^2}\hat{r} \tag{1-5}$$

When μ_0 is a constant $\mu_0=4\pi\times10^{-7}T\,m/A$

1. Therefore, the intensity of the Field of magnetism (B), could be found from the equation,

$$B=\frac{\mu_0}{4\pi}\int\frac{Id\ell\sin\theta}{r^2} \tag{1-6}$$

If there are other substances in the air around a magnetic field is always present because electric current flows within the circuit. Additionally, substances with inherent magnetism also generate a magnetic field due to their magnetization. Equation (1-7) was applicable solely to bodies immersed in a vacuum, as the presence of different materials alters the conditions. Various materials exhibit distinct magnetic permeability properties, influenced by the ratio of a substance's permeability (μ_0) to that of a vacuum. This is ratio termed relative magnetic permeability with (μ_r) highly magnetic substances possessing elevated relative values.

André-Marie Ampère was a scientist who experimented with the forces acting on electrical wires that carry electricity. Meanwhile, Michael Faraday was developing his Faraday's law by the late 1820s. Later, James Clerk Maxwell would combine the work of Faraday and Ampère to form four equations that could be viewed as the fundamentals of all electrical and electromagnetic phenomena. Maxwell's theory had a wider application than he realized, as in 1905 it agreed with the special theory of relativity. Maxwell's equation represents the previously discussed laws of electricity and magnetism. Although the equation also predicts the presence of electromagnetic waves which move at a speed of ($c = 1/\sqrt{\mu_0 \varepsilon_0} \approx 3 \times 10^8\, m/s$), Maxwell's equation demonstrated that such waves were emitted by an accelerating charge moving at a speed greater than that of light.

We provide recall Maxwell's equation in its simplest form here, that is without any dielectric or magnetic materials, or in free space. Here are the four equations:

$$\oint \vec{E} \bullet d\vec{A} = \frac{Q_{enc}}{\varepsilon_0} \quad (1\text{-}7)$$

$$\oint \vec{B} \bullet d\vec{A} = 0 \quad (1\text{-}8)$$

$$\oint \vec{E} \bullet d\vec{A} = -\frac{d\Phi_B}{dt} \quad (1\text{-}9)$$

$$\oint \vec{B} \bullet d\vec{A} = \mu_0 I_{enc} + \varepsilon_0 \mu_0 \frac{d\Phi_E}{dt} \quad (1\text{-}10)$$

I_{enc} is the current enclosed by the loop.

Φ_E/dt is the electric flux's rate of change.

Q_{enc} is the total charge enclosed within a volume.

Gauss's law, expressed in Equation (1-7), asserts that the net charge present inside any closed surface, divided by (ε_0), determines the total electric flux pass through that surface. According to this law an electric flow was related to a charge and ends on a negative charge (Halliday et al., 2007).

According to Equation (1-8), also referred to as Equation (1-10) and known as Gauss's law for magnetism, the net magnetic flux through a closed surface is zero. This means that the number of magnetic field lines entering and exiting a closed surface must be the same, indicating that magnetic field lines do not have distinct starting or ending points. If they did, it would imply the presence of isolated magnetic monopolies. Thus, Equation (1-8) is based on the principle that magnetic monopolies do not exist in nature.

Faraday's law of induction, as represented by Equation (1-9), describes the connection between an electric field and a changing magnetic flux. The law states that the rate of change of magnetic flux through any surface bounded by a closed loop is the integral line of the electric field around that loop, corresponding to the induced electromotive force (emf). One application of Faraday's law is the generation of current in a wire loop when exposed to a time-varying magnetic field.

Equation (1-10), representing the generalized form of Ampere's law, defines the relations between magnetic flux, electric currents, and electric fields. It states that the line integral of the magnetic field around any closed loop is determined by the sum of the net current passing through the loop and the rate of change of electric flux through the surface enclosed by the loop.

The force that a charged particle experiences in an electric and magnetic field is described by the Lorentz force equation, which is an important principle in electromagnetism. Given is the equation:

$$\vec{\mathrm{F}} = \mathrm{q}\left(\vec{\mathrm{E}} + \vec{v} \times \vec{\mathrm{B}}\right) \qquad (1\text{-}11)$$

When F is the Lorentz force acting on the particle in newtons (N).

q is the charge of the particle in coulombs (C).

E is the electric field in volts per meter (V/m).

v is the velocity of the particle in meters per second (m/s).

We identify with this as the Lorentz force, Maxwell's equation and this force law provides a comprehensive account of all conventional electromagnetic interaction.

1.2 The purpose of the research

1. To develop the demonstration laboratory kit of magnetic fields study on Ampere's Law.

2. To test the effectiveness of the magnetic field demonstration laboratory kit.

1.3 The importance of research

The development of a demonstration laboratory kit for studying magnetic fields had helped explain the behavior of magnetic fields generated by electrical currents, thereby enhancing our understanding of electromagnetic phenomena based on Ampere's Law.

1.4 Scope of the research

A demonstration laboratory set focused on studying magnetic fields had been developed using Ampere's law. The efficiency of the demonstration laboratory set had been studied by calculating the magnetic field using permeability and comparing it with the theoretical magnetic field. Additionally, efficiency had been studied by calculating the electric current and comparing it with the current measured by a multimeter and a clamp meter.

CHAPTER 2
LITERATURE REVIEW

Hans Christian Oersted's experiment revealed that an electric current flowing through a conductor generates a magnetic influence surrounding the conductor. The direction of this magnetic influence is influenced by the direction of the current, following the Ampère’s rule. The analysis of magnetic influence produced by currents typically focuses on two scenarios: the magnetic influence generated by a long, straight voltage-carrying wire and the magnetic influence produced by a voltage-carrying circular loop.

2.1 Magnetic fields produced by currents

In 1820, the Danish physicist Hans Christian Oersted found that an electric current flowing through a conductor creates a surrounding electromagnetic field. During an experiment in Copenhagen, Oersted discovered that placing a current-carrying wire atop a compass caused the needle to deviate perpendicular to the wire. The current flowing through the wire determined the direction of this deflection, which might be clockwise or counterclockwise. This established the existence of an electromagnetic field around the conductor when current is present, as depicted in Figure 6 (Griffiths, 2023).

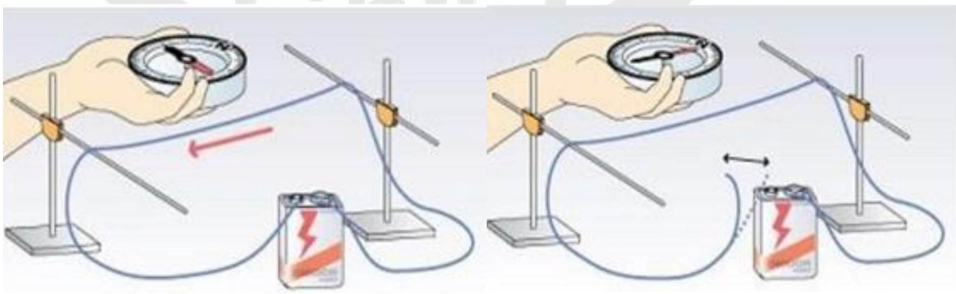

(a) (b)

Figure 6 Shows experiment of Hans Christian Oersted (a) When an electric current and (b) not electric current.

Source: (Griffiths, 2023)

From this phenomenon, another method could be used to visualize the Magnetic region: sprinkle metal filings onto a cardboard plate, then pass a current through the conductor wire positioned beneath the plate. Gently tap the cardboard, and you will observe that the iron filings are arranged into circular patterns, as illustrated in Figure 7.

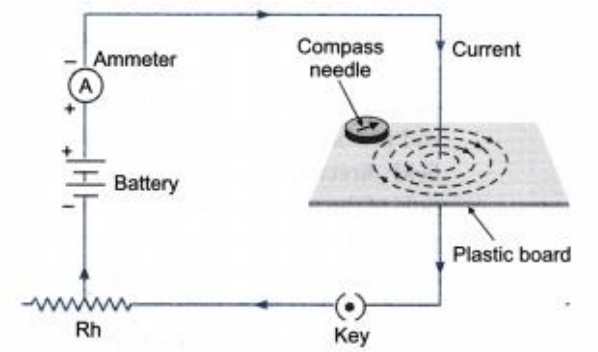

Figure 7 Observing magnetic region lines around an electrically conductive.

Source: (Griffiths, 2023)

The current-field direction rules help establish the relationship between the magnetic force around a conductor and the direction of the current. As per this rule, if you hold a current-carrying wire with your right hand and point your thumb in the direction of the current, your curled fingers will indicate the direction of the magnetic field lines around the conductor, as depicted in Figure 8 (Griffiths, 2023).

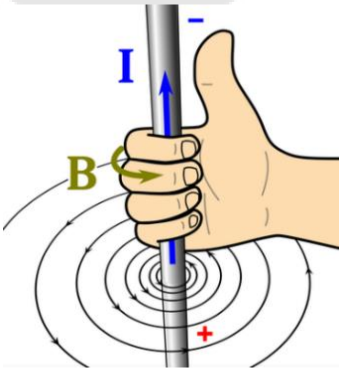

Figure 8 Right-hand rule of conductor.

Source: (Griffiths, 2023)

2.1.1 Magnetic fields created by a long straight current-carrying wire

Magnetic fields possess both possess both direction and magnitude. As discussed earlier, a compass can help determine the direction of a magnetic field. Figure 9 illustrates the magnetic field around a long, straight current-carrying wire. Using Hall probes, it is observed that the magnetic field forms circular loops around the wire. This finding prompted to the development of the thumb rule for current, applicable to any current segment: when the thumb points in the direction of the current, the fingers naturally curl in the direction of the field lines loops generated by the current (Griffiths, 2023).

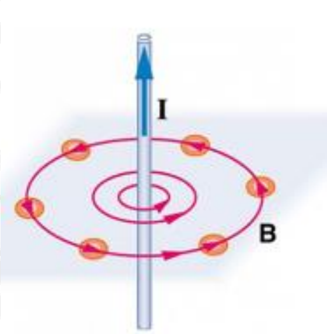

Figure 9 When a magnetic region is positioned next to a long, current-carrying wire compass placed nearby would change according to the strength of the magnet.

Source: (Griffiths, 2023)

2.1.2 Magnetic fields produced by an active conductor circular loop

The magnetic field lines around an active conductor could be observed, as illustrated in Figure 10, by inserting a wire through a cardboard or transparent plastic sheet and passing an electrical flow through it. To determine the size and direction of these magnetic lines, a compass can be placed at various points around the wire, and the deflection of the needle can be monitored. The needle's movement indicates the direction of the magnetic zone, as shown by the compass's north pole. When the current flows downward, the magnetic field lines circulate clockwise; if the current direction is reversed, the field lines switch to a counterclockwise orientation. In diagrams, arrowheads typically indicate the direction of electric current along the length of a cable.

In cross-sectional views, however, a cross symbol (×) represents current flowing away from the viewer, while a dot (•) indicates current flowing toward the viewer. When two conductors carrying current in the same direction are placed near each other, as shown, their magnetic fields align, creating an attractive force that pulls them together. Conversely, if the currents in the conductor's flow in opposite directions, the magnetic field lines become dense between them, resulting in a repulsive force that pushes them apart. Thus, two parallel wires with current flowing in the same direction will experience an attractive force, while those with current flowing in opposite directions will experience a repulsive force (Halliday et al., 2007).

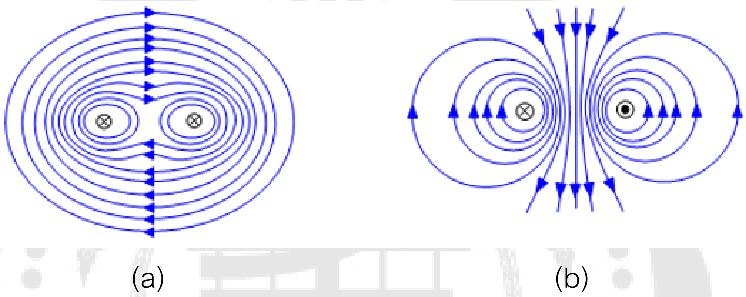

Figure 10 When two wires with current flowing in the same direction are placed close together.

Source: (Halliday et al., 2007)

2.2 Ohm's law and resistance

George Simon Ohm, a German physicist, discovers that the current flowing through a wire between two points is directly proportional to the voltage across those points, provided the temperature remains constant. This relationship is typically expressed as (Torbert et al., 2016).

$$V = IR \tag{2-1}$$

R is the resistance of the conductor in ohms (Ω).

V is the voltage across the conductor in volts, (V).

I is the current flowing through the conductors in amperes (A).

Ohm's Law explains that the current increases if the voltage at the source increases, and vice versa. If the power supply is constant, the current decreases with resistance. When multiple resistors are connected and treated as a single resistor, the electric resistance is called the combined resistance. There are 2 types of resistor connections: series and parallels connection (Samimi, Tenbohlen, Akmal, & Mohseni, 2016).

This equation shows that the peak current in an AC circuit is current multiplied by the square root of 2. This relationship is useful for converting between peak and RMS values, especially in power calculations for AC circuits.

$$I_{peak} = \sqrt{2}\, I_{rms} \tag{2-2}$$

I_{peak} represents the peak in an AC (alternating current) circuit.

I_{rms} stands for the root mean square (rms) current.

2.2.1 Resistors in series

Series circuits are also known as current circuits. In a series circuit, all components share the same current, meaning the current flowing through each part of the series connection is equal (Ling, Moebs, & Sanny, 2016).

In a series circuit, there is only one path for current to flow. If any connection in the circuit is broken or opened, the entire circuit will stop functioning. For example, in older-style Christmas tree light strings, the circuit becomes unusable until the faulty bulb is replaced if a single bulb burns out or is removed.

When 2 or more resistors are connected in any series, their combined resistance is the sum of their individual resistance.

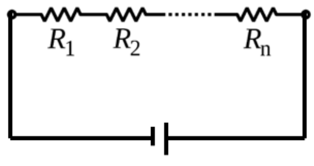

Figure 11 Connecting resistors in series.

Source: (Ling et al., 2016).

$$I = I_1 = I_2 = I_3 = \cdots = I_n \tag{2-3}$$

In a series circuit, the current is the same for all the elements.

$$V = V_1 + V_2 + V_3 \tag{2-4}$$

The voltage in one series circuit is the total of the voltage drops across each resistor unit.

$$R_{total} = R_s = R_1 + R_2 + R_3 + \cdots + R_n \tag{2-5}$$

Here, "series" is indicated by the subscript s in (R_s), while resistance in a series is indicated by (R_s).

2.2.2 Resistors in parallel

The parallel circuit, a potential difference (voltage) across the endpoints of all components is equal, with each component sharing the same polarity and experiencing the same potential difference. Every component connected in parallel receives a similar voltage. According to Kirchhoff's Current Law, the total current equals the combined sum of the currents passing through each individual component (Ling et al., 2016).

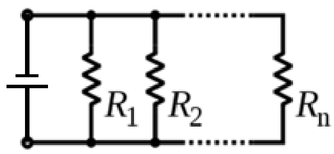

Figure 12 Connecting resistors in Parallel.

Source: (Ling et al., 2016).

Each element in a parallel circuit has the same voltage

$$V = V_1 = V_2 = V_3 = \cdots = V_n \tag{2-6}$$

Ohm's law may be used to find the current flowing through each individual resistor. Calculating the voltage factor gives

$$I_{total} = I_1 + I_2 + I_3 + \ldots + I_n \tag{2-7}$$

Add the reciprocals of the resistances to determine the total resistance of all the components.

$$\frac{1}{R_{total}} = \frac{1}{R_1} + \frac{1}{R_2} + \frac{1}{R_3} + \cdots + \frac{1}{R_n} \quad (2\text{-}8)$$

The unreciprocated expression is rather straightforward for only two resistances.

2.3 Smartphone sensors

Smartphones are personal possessions used by everyone for many hours a day (Dwyer, Kushlev, & Dunn, 2018). They serve as communication tools that resemble portable computers capable of connecting to various core functionalities, including those used by the police, such as various sensors integrated into the smartphone. Researchers (Khvorostianov, 2023; Matarboumosleh & Jaalouk, 2017) have provided the following definition: mobile applications are software that can offer additional benefits when used in conjunction with mobile devices. According to mobile applications combine the terms mobile and applications, where mobile refers to a portable communication device with basic features capable of functioning like a computer. It's a small, lightweight device capable of performing a variety of functions. Applications refer to software that users can employ to meet their needs. These mobile applications are designed for various operating systems, including Android, iOS, Windows smartphone, and others.

From the information above, mobile applications are programs that can be easily installed by users on various operating systems. They can increase the capabilities of mobile phones, enabling them to perform a wide range of functions like those of a computer. In this research, applications relying on sensors would be employed to measure the magnetic field that is installed inside the smartphone as an indicator of a strong magnetic field.

2.3.1 Smartphone sensor types

A sensor is a set of devices, circuits, or systems that measure changes in properties or the nature of things surrounding the target object. Sensors use enormous amounts of big data obtained from measurements to enter the distribution process, analyze the behavior of changes, and process it into knowledge and artificial intelligence (AI). This enables humans to use this knowledge to increase efficiency and reduce steps in the work process. Currently, sensor systems are used in various forms on mobile phones, such as the G-sensor, motion detection system, Accelerometer Sensor, automatic image rotation system, Orientation Sensor, screen angle adjustment sensor, sound level sensor, Magnetic Sensor (which measures magnetic field intensity), Light Sensor (which detects brightness for automatic adjustment of screen light), and Proximity Sensor (a system for automatically turning on/off the screen while talking on the phone). These features are often found in smartphone-style mobile phones, both in iOS and Android OS (Ramaneeya, 2016) sensor devices could be divided into 3 types according to their measurement properties, including:

- Physical Sensor is a sensor used to measure various physical properties. It uses special cells that are sensitive to light, temperature, motion, Field lines, gravity, humidity, vibration, pressure, electric fields, sound, and other physical characteristics of the external/internal environment, such as stretching force and organ movement. It also includes sensors for detecting toxins, nutrients, and a internal metabolic environment, such as sugar levels, oxygen levels, hormones, and neurotransmitters (Teh, Kempa Liehr, & Wang, 2020).

- Chemical Sensor is a sensor used to measure various chemicals. It relies on specific chemical reactions that are converted into data or signals that can be read and analyzed. Examples include sensors used to measure chemical contaminants in the environment, soil and water sensors, and equipment for analysis and testing. The development direction of equipment for analysis and testing tends to focus on sensors that are electronic tools capable of easily reading results. The results are displayed digitally or numerically, without the need for an expert to analyze and interpret them. Users can operate the device themselves. Due to the sensor's characteristics as a portable and easy-to-use analytical device, it has been applied in various industries.

- Biological sensors rely on using biological substances to produce specific reactions with target substances. Examples include sensors used to measure blood sugar levels (Zhao, Li, Zhou, & Zhang, 2016).

2.3.2 Smartphone Phyphox applications

The smartphone application (Magnetometer App) owned and developed by Phyphox was used to display data in an easily understandable format, facilitating quick and easy share across various platforms. Its main function, such as information display, relies on sensors in smartphones. It measured and displayed value data through numeric display tools, facilitating the visualization of measurements. This app, along with similar ones, could be downloaded free from the App or Play Store (Pierratos & Polatoglou, 2020; Staacks et al., 2022).

In this research, it relies on a magnetic intensity probe sensor that is installed in the smartphone, which detects characteristics of magnetic strength with a smartphone using a 3-axis measurement. The smartphone uses a magnetic intensity sensor head to measure the strength of magnets. Displays from applications that require a smartphone to tell various magnetic strength values from the display results to the smartphone screen automatically with the following steps for use: open the Phyphox, select sensor magnetometer, press start to save data in the Phyphox and graphs. When the data is saved, press stop and then send the data to Excel by selecting export data and choosing Excel, then clicking OK (Westermann, Staacks, Heinke, & Möhrke, 2022)

2.4 Related research

Williams (2014) measured the earth's local field lines using a Helmholtz coil. There was a point-like method for measuring the strength of the earth's local field lines. This activity could be done in most high schools by using this method. The Helmholtz coil needed to be leveled and positioned such that its axis was parallel to the earth's field lines horizontal component. As a result, in an absence of a current flow, the compass needle would point toward the northern close of the coil's axis and parallel to the compass, and students were very involved in the activity's setup, pushing themselves to perfect it to increase the precision of their measurements. Students put their electromagnetic knowledge to use while also becoming aware of the three-dimensional aspect of the earth's magnetic field. This exercise could be used as a typical electromagnetism laboratory exercise in an introductory physics course.

Tanawesh (2014) studied the development of scientific concepts regarding the field of magnetic-electric force by using a set of simple demonstration laboratory kit with multimedia. The group of samples consisted of 34 secondary school students in the academic year 2014, using a research design. Post-tests were administered to the sample group. The tools used in the research were activity sets together with multimedia and learning management plans. According to the scientific inquiry format, the test measured science concepts in the field of electromagnetic force at two levels. An interview tested science concepts and satisfaction, and measurement data were analyzed by finding the average. The research results showed that the sample group had higher ideas about magnetic fields after organizing the learning session. There was no significant statistical difference at the 0.05 level with the development of science concepts. Most students could explain science concepts well and had a positive attitude. They were satisfied with the learning management at a very good level. This indicates that inquiry-based learning management using activity sets, simple experiments combined with multimedia, can develop scientific concepts about electromagnetic fields. It is a way to create knowledge by oneself.

Enrique, Escobar, Suarez, Najera, and Beléndez (2015) used a smartphone to measure the magnetic field of small magnets, offering a very economical laboratory setup for introductory physics. This provided a low-cost laboratory exercise for the introductory physics course for any grade of sciences and engineering, which was well received by their students. The exercise involved using a smartphone (regardless of whether it ran on iOS, Android) along with a few small magnets. They used a magnetometer or magnetic field sensor with a free app that had to be downloaded and installed on the smartphone. The applications they utilized were magnetometer (iOS), magnetometer metal detector, and physics toolbox magnetometer. The setup was complete. The major goal of the exercise was for students to ascertain the relationship between component x of the magnetic field produced by various magnets, ranging from the common magnets found in refrigerators to ring magnets and spherical magnets. They discovered that the magnetic field's dependence on distance followed an x-3 relationship, which was completely consistent with the theoretical analysis. The second goal was to use the least squares fit method to determine this exponent, the magnetic moment of the magnets, and their respective absolute errors, as shown in Figure 13.

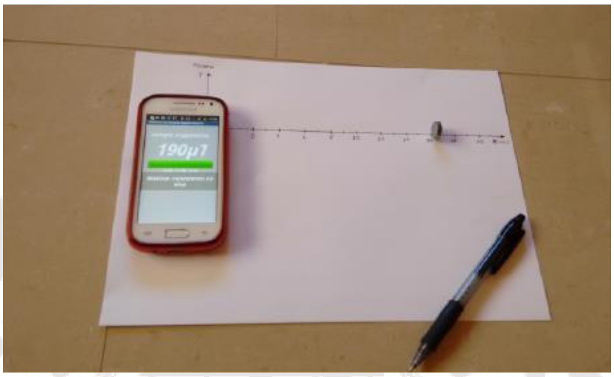

Figure 13 Experimental assembly in which you can perceive the small magnet and the smartphone.

Source: (Enrique et al., 2015)

Arabasi and Al-taani (2016) conducted an experiment to measurment the dip of the Earth's field lines using a smartphone, setting up a simple introductory physics laboratory experiment. Their paper introduced a smartphone-assisted apparatus that capitalized on the in-built magnetometer sensor of smartphones to determine the Earth's magnetic field dip angle. The primary objective of this setup was to assist students, particularly those at the high school and initial college levels, in visualizing the vectorial essence of the Earth's magnetic field, given that these students might not yet be well-acquainted with vector concepts. This apparatus served as a practical tool to bridge that knowledge gap. Furthermore, the affordability, user-friendliness, and ease of production of this setup made it an ideal instructional aid that could be readily assembled by physics educators at both high schools.

Pili and Violanda (2018) conducted an experiment measuring the mean angular velocity with a smartphone magnetic sensor. With the pervasive presence of smartphones in the contemporary educational environment, their multifunctional sensors offered a plethora of opportunities for hands-on experimentation in physics education. The study presented a novel methodology to measure the average angular velocity utilizing the magnetic field sensor embedded in smartphones. This was done by attaching a small magnet to a rotating object and placing the smartphone proximate to its rotational path. The magnetometer captured variations in magnetic field strength corresponding to the object's rotations. By analyzing these variations, the who were able to deduce the average angular velocity of the rotating object. The results demonstrated a high degree of accuracy when juxtaposed with conventional angular velocity measuring instruments. The cost-effectiveness, accessibility, and precision of this method underscored its potential as an invaluable tool in pedagogical settings, emphasizing the transformative capability of smartphones in enriching physics experiments.

Salvatore, Enrico, Daniela, and Melda (2019) used a mobile phone's magnetic sensor in a low-cost experiment to study the field magnetic due to Helmholtz and anti-Helmholtz coils in the realm of magnetostatics experimentation. Accurately measuring magnetic fields was pivotal. Their paper introduced an innovative method for measuring the magnetic field generated by a current-carrying coil, deploying the embedded magnetic sensor in smartphones as a viable alternative to the more costly magnetic sensor probes traditionally used. The precise location of the smartphone's magnetic sensor was determined by mapping the magnetic field values of a permanent magnetic bar, ensuring the fidelity of measurements. Their investigation adjusted two primary parameters: Interrelation of the coil and the smartphone's magnetic sensor and the current's magnitude circulating through the coil. The coil utilized in this study had a radius of 8 cm, encompassed 30 wire of turns, and had a current of 0.3 A. For experimental variations, the coils were set in both Helmholtz and anti-Helmholtz configurations. The magnetic fields resulting from a solitary coil, Helmholtz coil, and anti-

Helmholtz coil were diligently measured. These measurements were then juxtaposed with values derived from both analytical and numerical calculations. The outcomes affirmed that the smartphone's magnetic sensor could precisely measure the Field of magnetism produced by both Helmholtz and anti-Helmholtz coils, showcasing its potential utility in physics experiments, as illustrated in Figure 14.

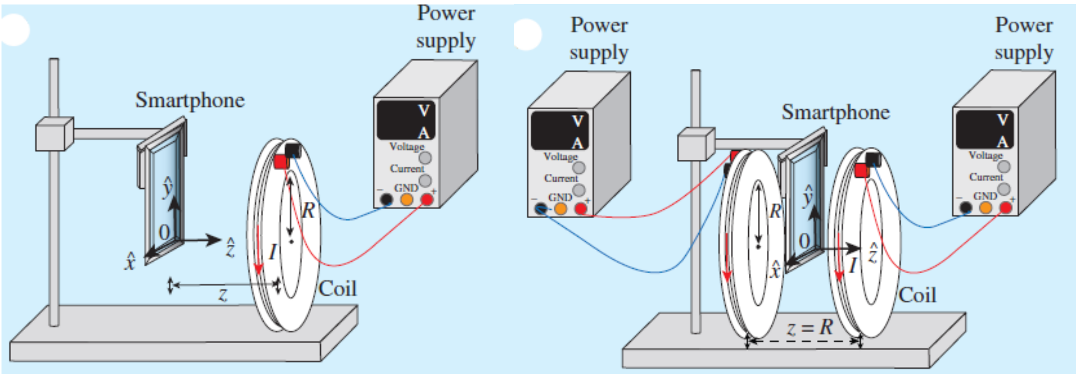

(a) (b)

Figure 14 Measurement configuration of the magnetic field due to (a) one coil and (b) two coils.

Source: (Salvatore et al., 2019)

Arribas et al. (2020) studied the measurement of the magnetic field using a smartphone. A method for quantifying the magnetic field generated by linear quadruplets is described. They used two different magnets: (a) a neodymium ring with a diameter of 3.5 cm and (b) a ceramic magnet with a diameter of 1.5 cm. Using a smartphone as a device to measure magnetic strength, the experiment revealed magnetic intensity patterns based on the distance between the magnet and the smartphone. As the distance between the magnet and the smartphone increased, the magnetic intensity noticeably decreased. The two candidates tested, neodymium magnets and ceramic magnets, were evaluated using the same method. The results showed that neodymium magnets consistently produced higher intensity compared to ceramic magnets, as in Figure 15.

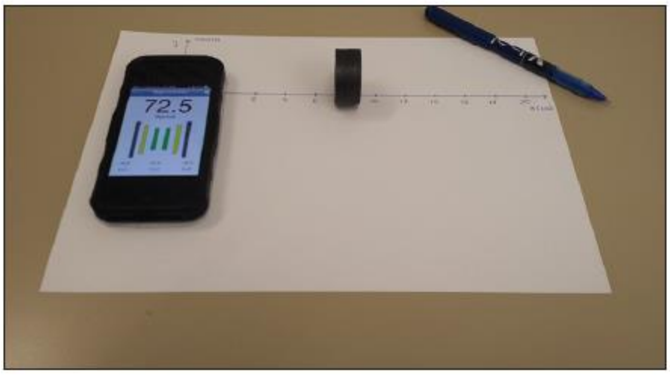

Figure 15 The mobile phone is placed on a sheet of paper for the experiment.

Source: (Arribas et al., 2020)

Carroll and Lincoln (2020) used smartphones with the Phyphox app to teach physics in the classroom. The Phyphox app utilized the sensors already built into smartphones to provide real-time data and graphs. Generally, a wide range of experiments were available through the app, offering unique opportunities for learning. While this feature was common among mobile physics apps, Phyphox was highlighted as particularly useful in some publications of this journal. Additionally, Phyphox was open source, allowing users to go beyond the built-in experiments. Teachers and students could unleash their imagination and creativity with this app, which also worked with Arduino. Furthermore, the app could remotely connect to PCs to transmit live data.

Pathak and Patel (2022) created an analysis of a free-falling magnet to determine gravitational acceleration using a smartphone's magnetometer. This work was conducted in contemporary physics education, where the integration of smartphones as investigative tools was progressively becoming prominent due to their accessibility and the multitude of sensors they housed. They introduced an innovative approach to measure gravitational acceleration by analyzing a free-falling magnet, leveraging the magnetometer sensor in smartphones. They presented a setup for an experiment in which a magnet was set to fall freely while the magnetometer on a smartphone recorded the different magnetic field strengths. Magnitude changes of the magnetic area were found to be correlated with the acceleration of the magnet caused by gravity through further data analysis. The method's effectiveness and potential were highlighted by the preliminary results, which showed a strong agreement with the standard value of gravitational acceleration. This study demonstrated the revolutionary impact of smartphones on contemporary physics education in addition to offering a new, affordable, and easily accessible method for measuring gravitational acceleration, as shown in Figure 16.

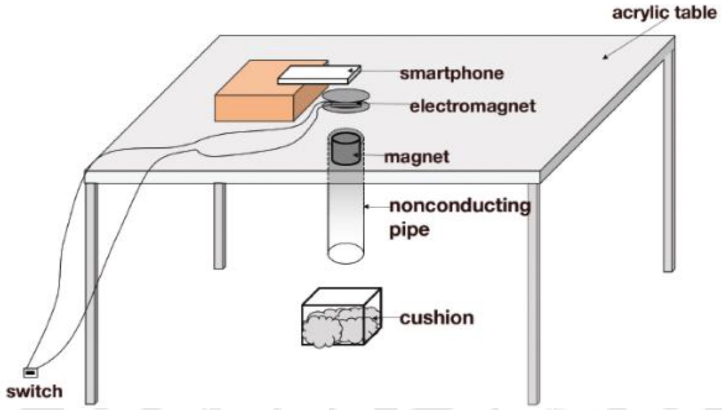

Figure 16 Table experimental setup to calculate acceleration due to gravity.

Source: (Pathak & Patel, 2022)

Wannous and Horvath (2023) made accurate measurements using a smartphone magnetometer, measuring magnetic fields and permeability discussed a method for measuring permeability in high school physics classes using a smartphone's magnetometer. Smartphone sensors, including magnetometers, have gained popularity in classrooms, and this article explored their use in physics education. The focus was on measuring the magnetic field of a coil with negligible length, which could be easily created using simple materials and could accommodate a smartphone inside it. To use the smartphone's magnetometer accurately, it was crucial to determine its location on the device, which could be done using a suitable compass app. The article described an experiment where a smartphone was placed inside the coil, and the magnetic field was measured as the current intensity was varied. This data has been used to determine the relationship between the magnetic field, the intensity of the current, and the number of coils turned. The permeability of a vacuum was calculated based on the measured data, providing a practical approach to teaching this concept. The article also explored the possibility of applying the same technique to measure the tangential component of Earth’s magnetic field, highlighting different experimental setups and factors to consider for accurate measurement.

The wire generates a magnetic area around it, following the direction given by the Ampere Law: if you curl your fingers around the wire while pointing your thumb in the direction of the current, your fingers indicate the magnetic field’s direction. Magnetic materials wrapping around wire align with the direction of your curled fingers. This setup uses small compasses to display the magnetic field direction at specific points along the wire. When no current flows, all compasses point north, aligning with Earth's magnetic south pole. However, a limitation of this design is that it does not provide a clear demonstration because the compasses are influenced by both the vertical and horizontal components of the magnetic field.

The article presents a practical and cost-effective way to measure permeability in a high school physics course using a smartphone's magnetometer, making it accessible for both students and teachers. It highlights the versatility of smartphone sensors in physics education.

CHAPTER 3
RESEARCH METHODOLOGY

In this study, we designed a demonstration laboratory kit to measure the magnetic area around a straight electrical wire using the Phyphox smartphone app. We also assessed the effectiveness of this experimental setup for both educational and practical applications. This chapter details the preparation of the demonstration kit and describes the experimental procedures, which are divided into 2 sections: Part 1 involves measuring the magnetic field produced by current in a single straight wire, while Part 2 focuses on measuring the AC current in household electrical appliances.

3.1 Experiment preparation

3.1.1 Materials and equipment

Table 1 Materials, equipment, and their usage.

Materials / Equipment	Their usage
1. Smartphone 	We used an iPhone 7 Plus with the Phyphox app installed to measure the magnetic field.
2. Digital Multimeter 	We used the Sanwa RD701 digital multimeter to measure the current and electrical potential in the circuit.
3. Power Supply 	We used a power supply with a 220 V AC input and a 12 V AC output.

Table 1(Next) Materials, Equipment, and Their Usage.

Materials / Equipment	Their usage
4. Resistor 	We used 5-ohm, 20-watt resistors to control and adjust the current and voltage in the electrical circuit.
5. Compass 	We used a compass to indicate the directions of north and south.
6. Spirit Level 	The spirit level is a device used to check whether the surface is level.
7. Clear Acrylic 	We created a table from clear acrylic, which is lightweight, strong, durable, easy to move, and can be molded into various shapes as desired.

3.1.2 Magnetic sensor position in smartphones

The location of the magnetic sensor in smartphones was determined primarily by observing the sensor's response to a nearby magnet. When a magnet was placed near the sensor, it triggered changes in the sensor's conditions, such as variations in resistance or signal frequency. These changes served as indicators for detecting and locating the sensor. The following steps were used to identify the magnetic sensor's location in smartphones:

1) Draw a grid on a sheet of paper with 2-millimeter spacing.

2) Set the origin of the X-Y axis at point (0,0).

3) Position the magnet at (0,0).

4) To pinpoint the sensor's location, open the app of Phyphox and move the smartphone along the X and Y axes. The sensor is located where the magnetic intensity is highest.

An inspection of the magnetic sensor location on the iPhone 7 Plus, as shown in Figure 17 (a), reveals that the sensor is positioned near the smartphone's front camera, as displayed in Figure 17 (b).

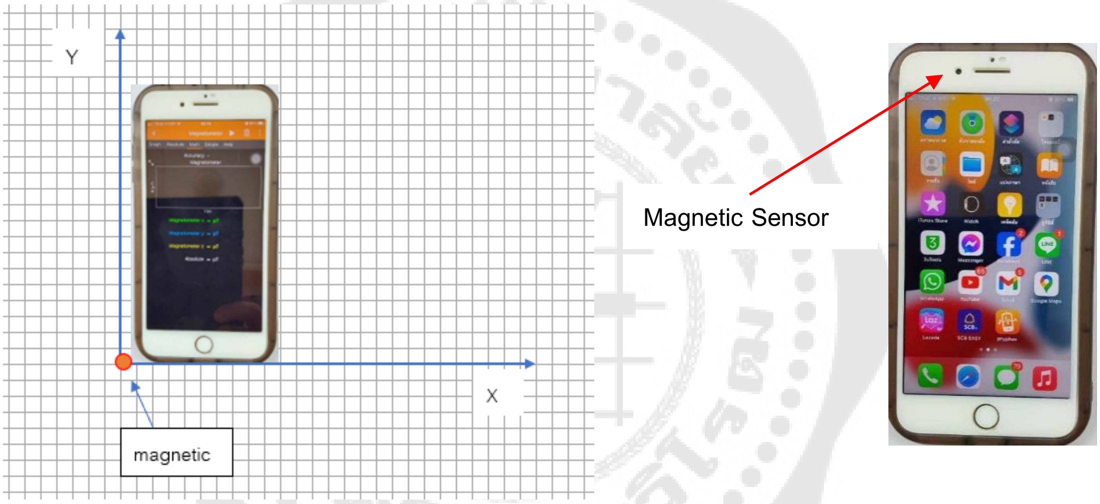

(a) (b)

Figure 17 (a) Verification of the sensor location (b) The magnetic sensor positioned near the front camera.

3.2 Design and creation of a demonstration laboratory kit

3.2.1 Demonstration kit table

1) Table design a demonstration kit table with dimensions of 600 mm x 600 mm x 7 mm (wight x length x thickness), positioned 300 mm above the floor. Stretch a straight wire connected to a binding post, as displayed in Figure 18.

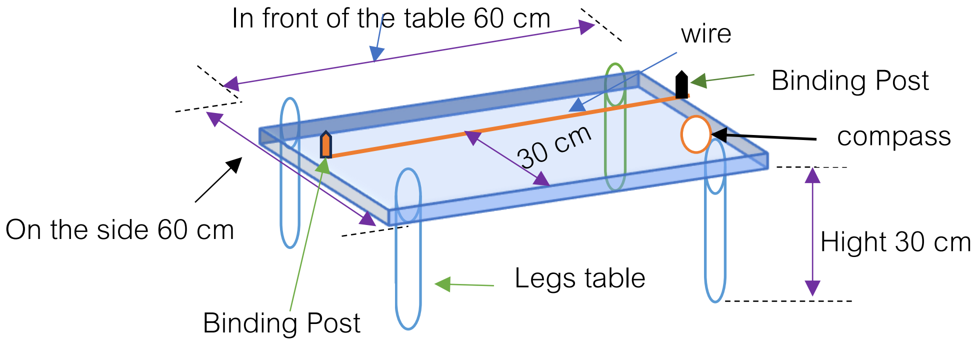

Figure 18 The acrylic table used for this experiment.

2) Table Assembly: Construct the table from acrylic following the design in Figure 18. The steps are as follows:

- Cut two acrylic sheets into rectangles with dimensions of 600mm x 600 mm x 6 cm and 600 mm x 600 mm x 1 mm.

- Stretch a straight wire and connect it to a binding post positioned in the center of the 6 mm thick acrylic sheet. Then, draw a grid with 2 mm x 2 mm lines, as shown in Figure 19.

- Place the 1 mm thick acrylic sheet on top of the 6 mm thick acrylic sheet, layering them together.

- Cut four cylindrical acrylic rods, each 30 cm in height, to serve as table legs. Assemble these legs with the layered acrylic sheets from step 3 to form the experimental table, as shown in Figure 19.

Figure 19 The acrylic table used in this experiment.

3.2.2 Circuit design in the demonstration kit

We measured the magnetic field generated by a straight wire. In Case 1, an alternating current (AC) circuit related to a single 5-ohm resistor, as shown in Figure 20. In Case 2, two 5-ohm resistors were connected in series, as shown in Figure 21. In Case 3, three 5-ohm resistors were connected into series, as shown in Figure 22. In Case 4, two 5-ohm resistors were connected in parallel, as depicted in Figure 23. Finally, in Case 5, three 5-ohm resistors were Interconnected in parallel, as illustrated in Figure 24.

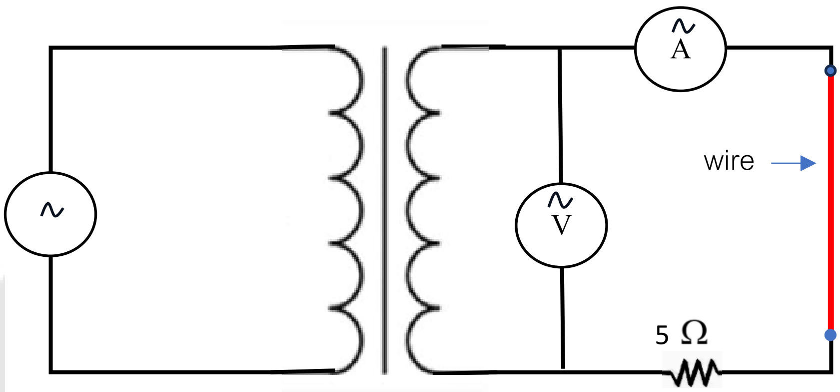

Figure 20 An electrical circuit containing a single resistor.

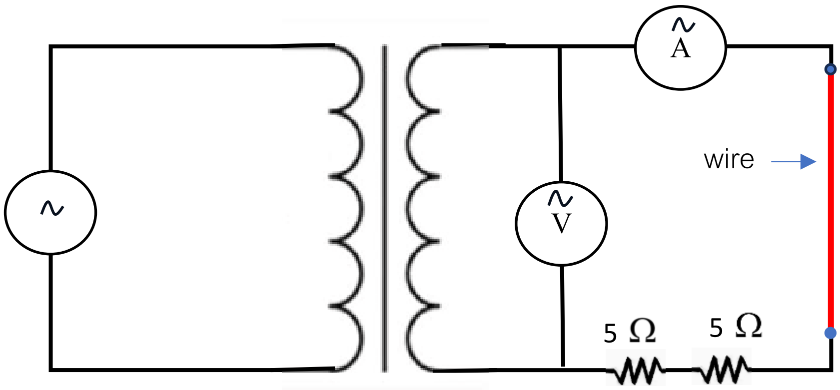

Figure 21 An electrical circuit with 3 resistors connected in series.

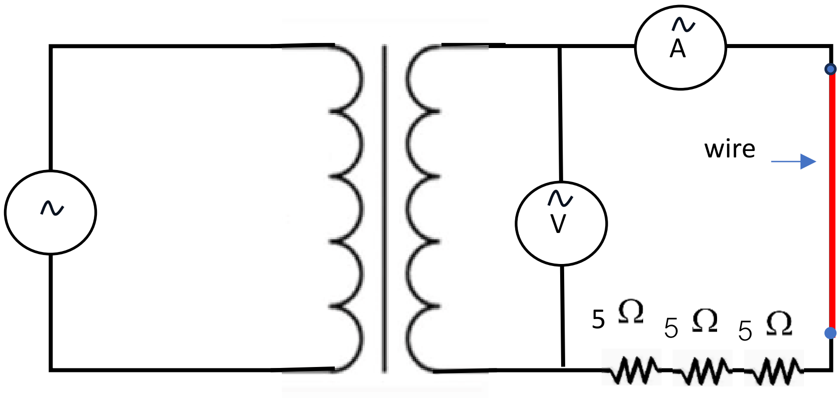

Figure 22 An electrical circuit such as 3 resistors connected in series.

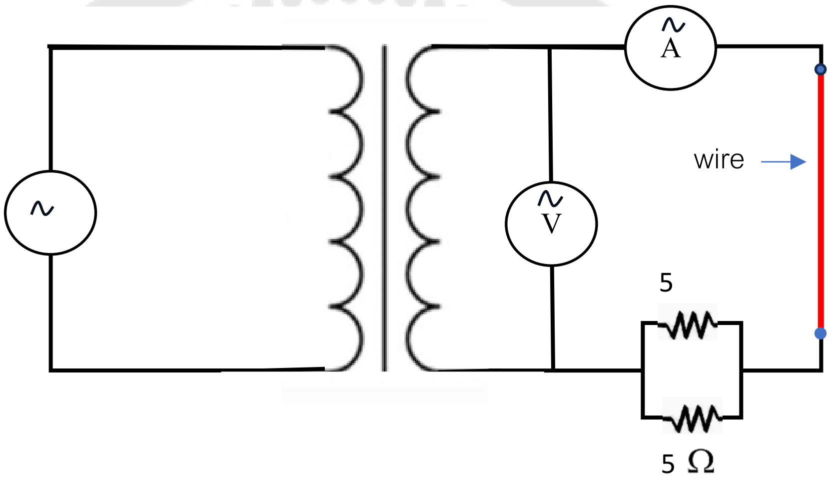

Figure 23 An electrical circuit including 2 resistors connected in parallel.

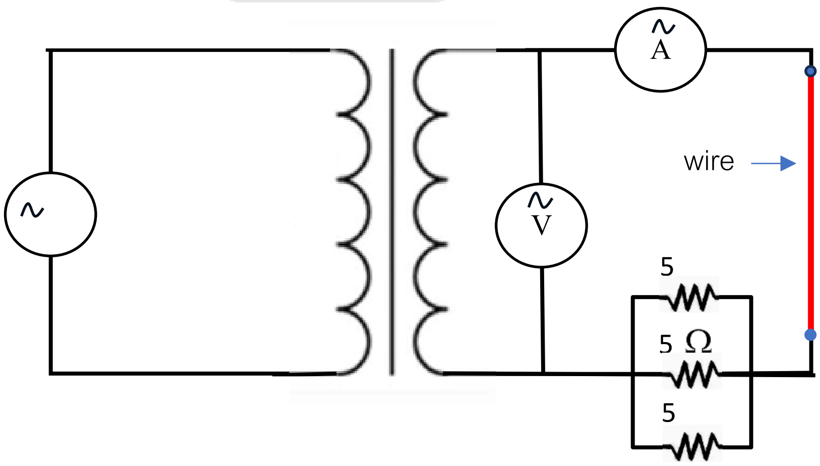

Figure 24 An electrical circuit with three resistors connected in parallel.

3.3 Applications used in the experiment

The Phyphox application, version 1.1.5, was developed in 2016 by the Institute of Physics at RWTH Aachen University in Germany. Dr. Sebastian Staacks and Prof. Christoph Stampfer were the principal inventors and developers, with Dominik Dorsel, Jonas Gessner, and Camilla Lummerzheim as key programmers. Phyphox enables continuous measurement and recording of various physical quantities across all three axes (x, y, and z), including linear acceleration, angular velocity, magnetic field intensity, and luminosity. The app also offers multiple experimental functions, such as sound and mechanics experiments, utilizing the smartphone's built-in sensors. Phyphox can simultaneously engage multiple sensors—such as the accelerometer, magnetic field sensor, gyroscope, and ambient light sensor—displaying the results as graphs or numerical values on-screen, as shown in Figure 25. Additionally, it includes a remote-control function, enabling users to control the app from multiple devices concurrently, and allows data files to be shared via email or other channels for further analysis. Phyphox is freely available on both iOS (The App Store) and Android (Google Play) (Nazar, Jiao, Zhang, Egbe, & Alavi, 2021).

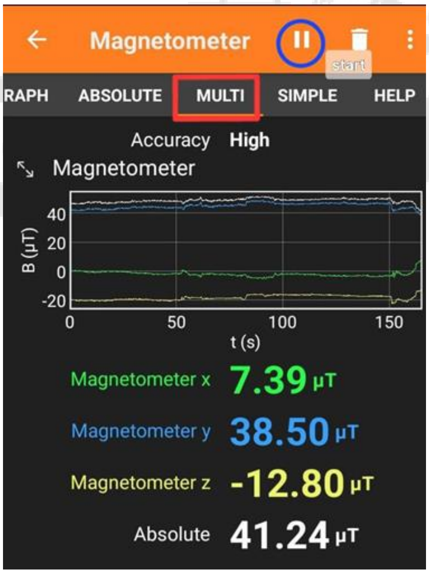

Figure 25 Displays the Phyphox application in use on a smartphone.

3.4 Experimental method

1) Calibration of the table: The table was leveled using a spirit level to ensure a flat surface across all points. It was then aligned precisely along a North-South axis using a straight edge and compass for accurate orientation. Precautions were taken, as improper leveling of the table could distort the experiment, and misalignment of the table and smartphone could also affect results due to potential interference from the geomagnetic field.

2) Measuring the magnetic field generated by the current in a single straight wire: The setup, illustrated in Figure 26, involved connecting a straight wire to a binding post located at the center of the experimental table. The smartphone was then positioned carefully to ensure the magneto sensor was placed in the optimal location for accurate measurement of the magnetic field.

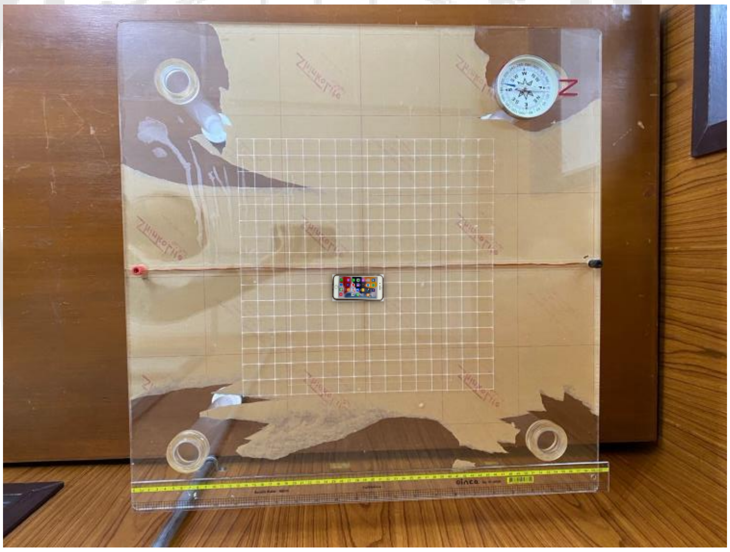

Figure 26 The smartphone was positioned 1–8 cm away from the wires.

- We used Case 1, an alternating current (AC) circuit connected with a single 5-ohm resistor, and began measuring the magnetic field on the left side of the coil, starting at a distance of 1 cm and continuing to 8 cm.
- We used Case 2 (two resistors in series), Case 3 (three resistors in series), Case 4 (two resistors in parallel), and Case 5 (three resistors in parallel) and measured

the magnetic field from 1 cm to 8 cm on both the right and left sides of the coil for each case.

- Analyze the relationship between time and magnetic field intensity, as well as a relationship between magnetic field intensity and the inverse of the distance from the coil for all cases, and determine the slope from the resulting graphs.

- Use Ampère's Law to calculate the magnetic permeability for each case and compare the results with standard values.

3) Measuring the AC current in the electrical appliance: The procedure and components are illustrated in Figure 27. Position the smartphone perpendicular to the north-south axis, at distances of 10 mm and 20 mm from the wire.

- We measured the magnetic field in a circuit connected to an electrical appliance using four different configurations, with measurements taken at distances of 1 cm and 2 cm for each configuration.

- Analyze the graph depicting the relations between the magnetic field and AC current. Calculate the average current for each case and compare it with the values measured by the multimeter and clamp meter.

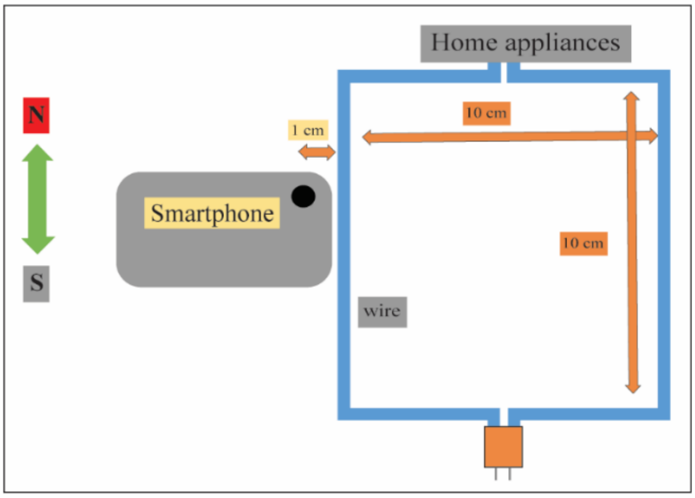

Figure 27 The diagram of the experiment setup.

CHAPTER 4
RESULTS AND DISCUSSIONS

In this research, we measured the magnetic field using the Phyphox application on a smartphone, dividing the study into two main parts: 1. measuring the magnetic field produced by the current in a single straight wire and 2. measuring the AC current in electrical equipment. For the first part, we measured the magnetic field at eight points to the left and eight points to the right of the wire, with each point spaced 1 cm apart. The circuit included five configurations of a 5-ohm, 20-watt resistor: Case 1 – a single resistor, Case 2 – two resistors in series, Case 3 – three resistors in series, Case 4 – two resistors in parallel, and Case 5 – three resistors in parallel. In the second part, we measured the magnetic field in a circuit connected to electrical appliance and measured the current using a multimeter and clamp meter.

4.1 Measuring the magnetic field produced by the current in a single straight wire

We used the magnetometer feature in the Phyphox application on an iPhone 7 Plus to measure the magnetic field at distances of 1 cm to 8 cm from the straight wire, on both the left and right sides.

4.1.1 Case 1: A single resistor

We set up an AC circuit using a 5-ohm, 20-watt resistor. The measured root means square current $\left(I_{rms}\right)$ was 1.400 A. Then, we calculated the peak current using the formula $I_{peak} = \sqrt{2}\, I_{rms}$, resulting in a peak current $\left(I_{peak}\right)$ of 1.974 A. Based on the data obtained from the magnetometer, we used Microsoft Excel 365 to display the relationship between magnetic field intensity and time, as shown in Figure 28. In this figure, (a) represents the magnetic field intensity on the left side of the coil, and (b) represents the intensity on the right side. We applied an equation $B_x = \left(\frac{B_{\max} - B_{\min}}{2}\right)$ to calculate the magnetic field intensity along the x-axis at distances from 1 cm to 8 cm from the coil. The results are presented in tables, with Table 2 showing the magnetic field intensity on the left and right sides of the coil. Additionally, Figure 29 illustrates an relationship between the magnetic field intensity along the x-axis $\left(B_x\right)$ and an inverse of the distance from the coil $\left(\frac{1}{r}\right)$, where (a) shows the intensity on the left side of the coil, and (b) shows the intensity on the right side.

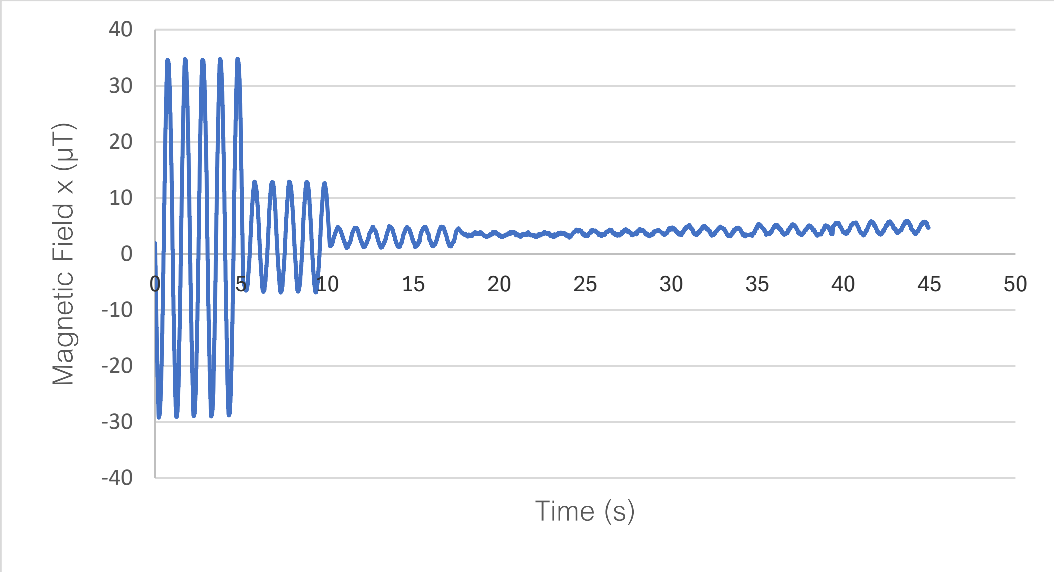

(a)

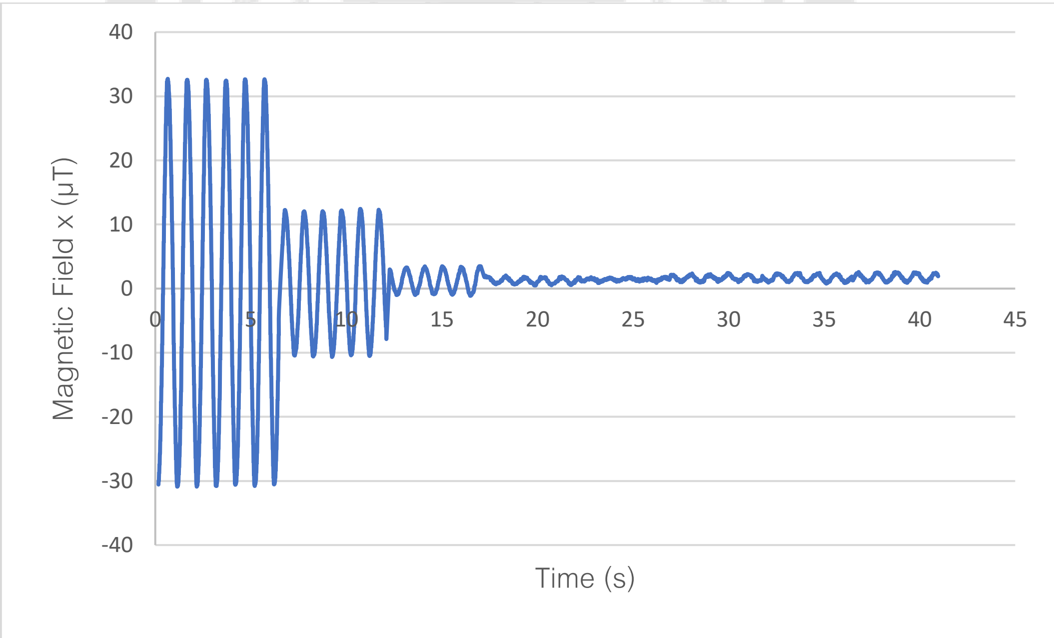

(b)

Figure 28 The relationship between magnetic field intensity and time for Case 1: (a) on the left side of the coil and (b) on the right side of the coil.

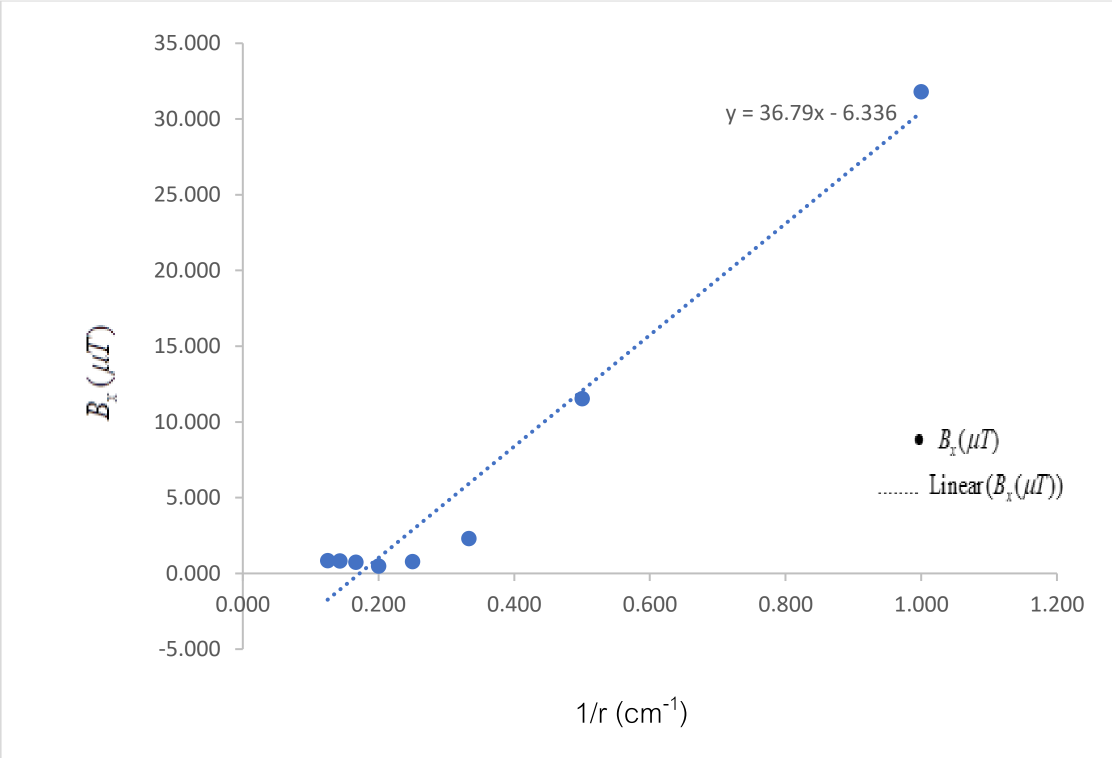

(a)

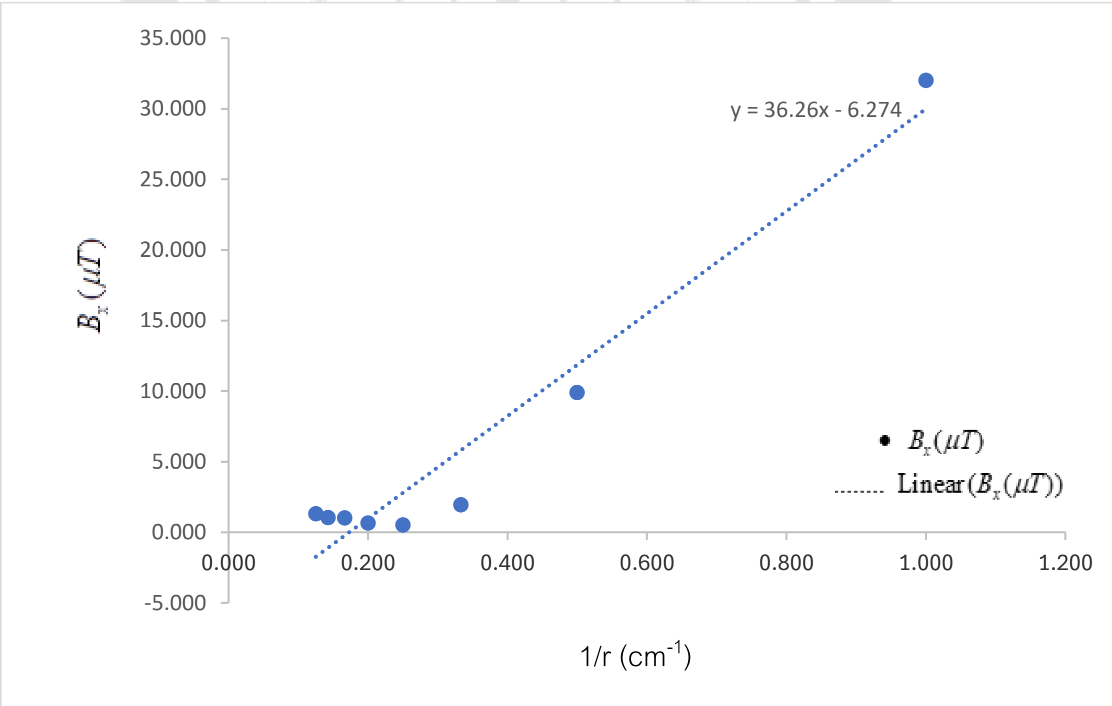

(b)

Figure 29 The relationship between the magnetic field intensity and the inverse of the distance from the coil for Case 1: (a) on the left side and (b) on the right side.

Table 2 The magnetic field intensity for Case 1 on the left and right sides of the coil.

$r\ (cm)$	$\frac{1}{r}\ (cm^{-1})$	$B_{x(Left)}\ (\mu T)$	$B_{x(Right)}\ (\mu T)$
1	1.000	32.00	31.80
2	0.500	9.890	11.54
3	0.333	1.952	2.302
4	0.250	0.514	0.769
5	0.200	0.655	0.484
6	0.167	1.007	0.736
7	0.143	1.044	0.829
8	0.125	1.300	0.839

From the relationship graph in Figure 29, parts (a) and (b), the slopes were found to be $36.26\times10^{-8}T\cdot m$ and $36.79\times10^{-8}T\cdot m$, respectively. Using Ampere's law, $B=\frac{\mu_0 I}{2\pi r}$, the magnetic permeability of vacuum was calculated to compare with the standard magnetic permeability of vacuum $\left(\mu_0=1.256\times10^{-6}\ N\cdot A^{-2}\right)$. Given that the slope from the relationship graph is defined as $slope=\frac{\Delta B}{\Delta\left(\frac{1}{r}\right)}$, it follows that $\mu_{Calculate}=\frac{slope\ 2\pi}{I_{peak}}$. The calculated magnetic permeability of vacuum $\left(\mu_{Calculate}\right)$ were $1.153\times10^{-6}N\cdot A^{-2}$ and $1.170\times10^{-6}N\cdot A^{-2}$, with percent errors of 9.643% and 7.957%, respectively, when compared to the standard value.

4.1.2 Case 2: Two resistors in series

We set up an AC circuit with two 5-ohm, 20-watt resistors connected in the series. The measured root means square current $\left(I_{rms}\right)$ was 0.800 A. Then, we calculated the peak current using the formula $I_{peak}=\sqrt{2}\,I_{rms}$, resulting in a peak current $\left(I_{peak}\right)$ of 1 .128 A. Based on the data obtained from the magnetometer, we used Microsoft Excel 3 6 5 to display the relationship between magnetic field intensity and time, as shown in Figure 30. In this figure, (a) represents the magnetic field intensity on the left side of the coil, and (b) represents the intensity on the right side. We applied the equation $B_x = \left(\frac{B_{max} - B_{min}}{2}\right)$ to calculate the magnetic field intensity along the x-axis at distances from 1 cm to 8 cm from the coil. The results are presented in tables, with Table 3 showing the magnetic field intensity on the left and right sides of the coil. Additionally, Figure 31 illustrates the relationship between the magnetic field intensity along the x-axis (B_x) and the inverse of the distance from the coil $\left(\frac{1}{r}\right)$, where (a) shows the intensity on the left side of the coil, and (b) shows the intensity on the right side.

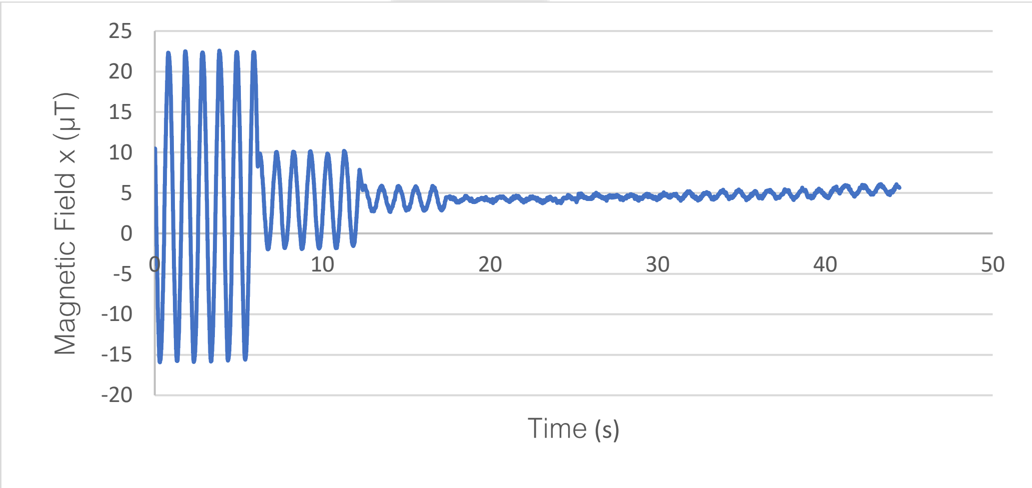

(a)

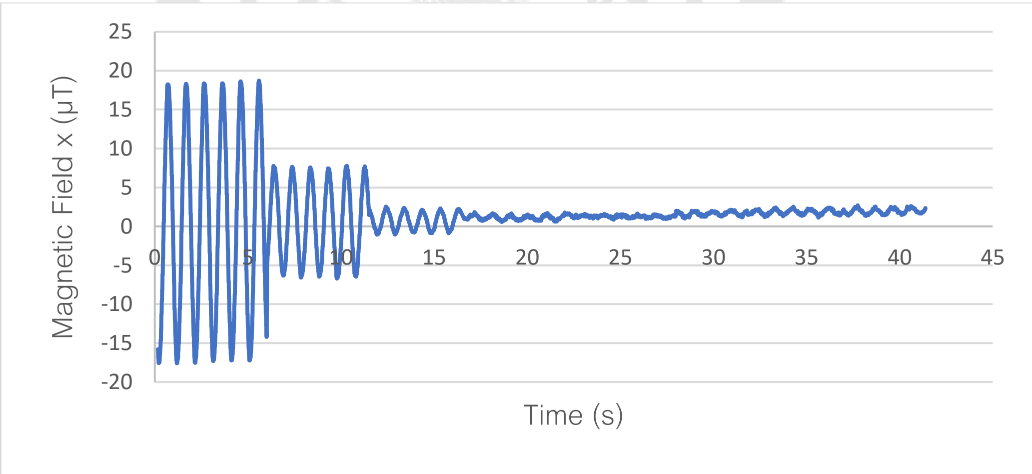

(b)

Figure 30 The relationship between magnetic field intensity and time for Case 2: (a) on the left side of the coil and (b) on the right side of the coil.

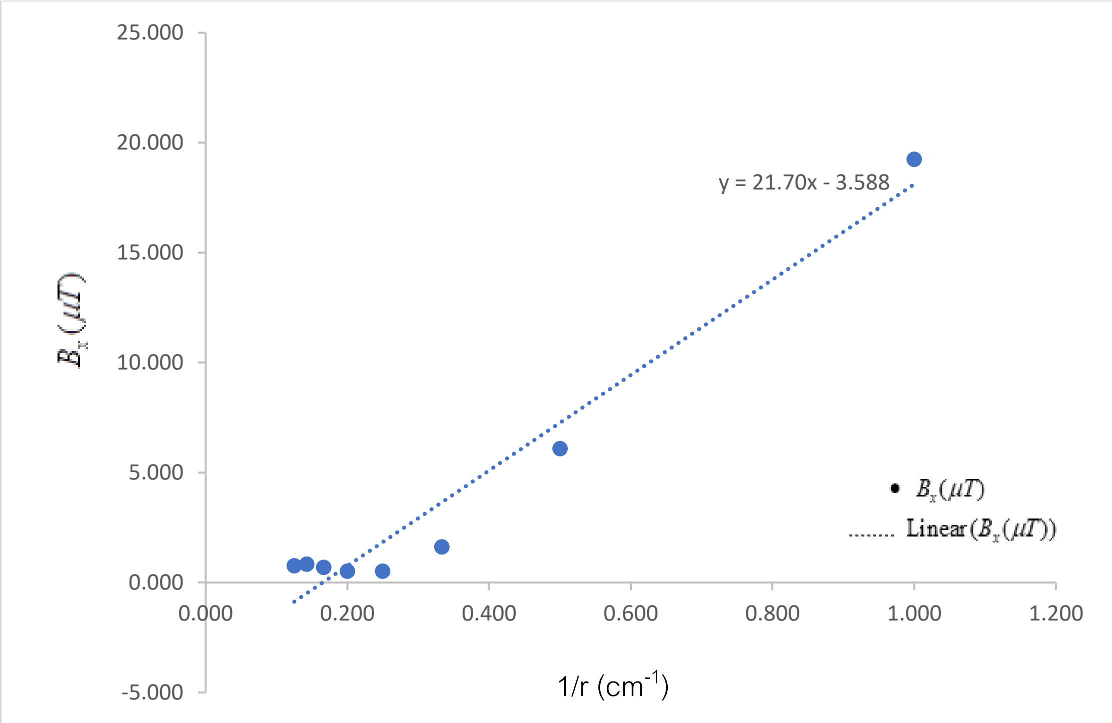

(a)

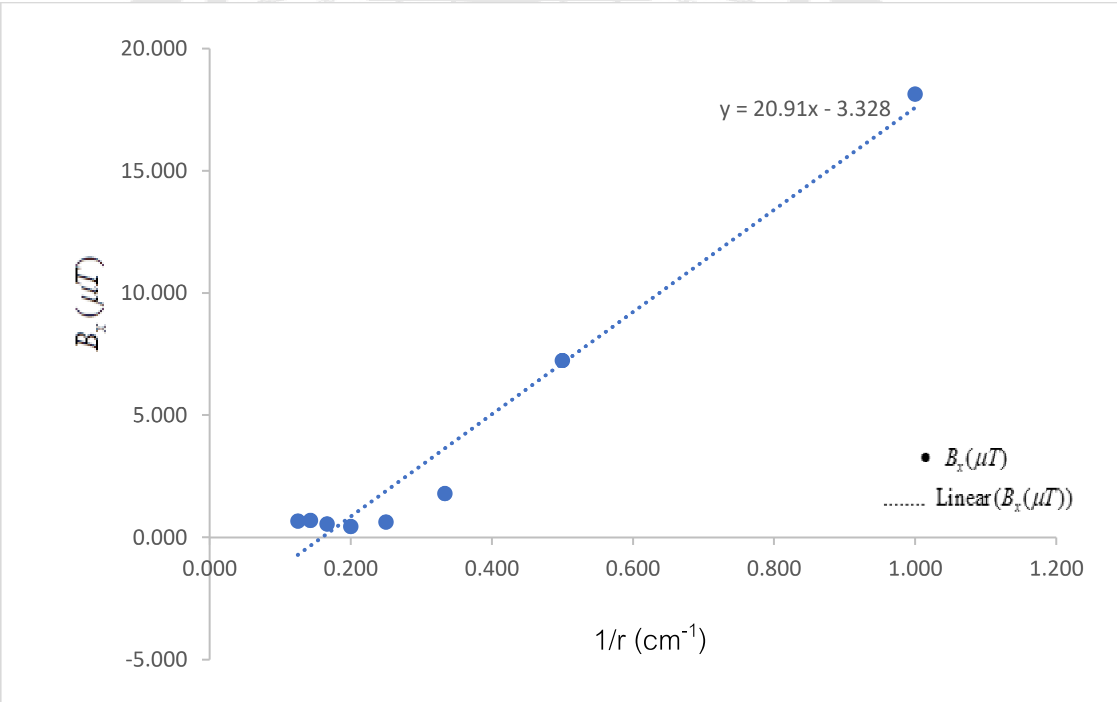

(b)

Figure 31 The relationship between the magnetic field intensity and the inverse of the distance from the coil for Case 2: (a) on the left side and (b) on the right side.

Table 3 The magnetic field intensity for Case 2 on the left sides and right sides of the coil.

$r\ (cm)$	$\frac{1}{r}\left(cm^{-1}\right)$	$B_{x(Left)}\left(\mu T\right)$	$B_{x(Right)}\left(\mu T\right)$
1	1.000	19.25	18.14
2	0.500	6.082	7.239
3	0.333	1.626	1.801
4	0.250	0.513	0.633
5	0.200	0.519	0.456
6	0.167	0.692	0.560
7	0.143	0.828	0.697
8	0.125	0.763	0.673

From the relationship graph in Figure 30, parts (a) and (b), the slopes were found to be $21.70\times10^{-8} T\cdot m$ and $20.91\times10^{-8} T\cdot m$, respectively. The calculated magnetic permeability of vacuum $\left(\mu_{Calculate}\right)$ were $1.153\times10^{-6} N\cdot A^{-2}$ and $1.153\times10^{-6} N\cdot A^{-2}$, with percent errors of 4.187% and 8.586%, respectively, when compared to the standard value.

4.1.3 Case 3: Three resistors in series

We set up an AC circuit with three 5-ohm, 20-watt resistors connected in series. The measured root means square current $\left(I_{rms}\right)$ was 0.550 A. Then, we calculated the peak current using the formula $I_{peak}=\sqrt{2}\,I_{rms}$, resulting in a peak current $\left(I_{peak}\right)$ of 0.775 A. Based on the data obtained from the magnetometer, we used Microsoft Excel 365 to display the relationship between magnetic field intensity and time, as shown in Figure 32. In this figure, (a) represents the magnetic field intensity on the left side of the coil, and (b) represents the intensity on the right side. We applied the equation $B_x=\left(\frac{B_{max}-B_{min}}{2}\right)$ to calculate the magnetic field intensity along the x-axis at distances from 1 cm to 8 cm from the coil. The results are presented in tables, with Table 4 showing the magnetic field intensity on the left and right sides of the coil.

Additionally, Figure 33 illustrates the relationship between the magnetic field intensity along the x-axis (B_x) and the inverse of the distance from the coil $\left(\frac{1}{r}\right)$, where (a) shows the intensity on the left side of the coil, and (b) shows the intensity on the right side.

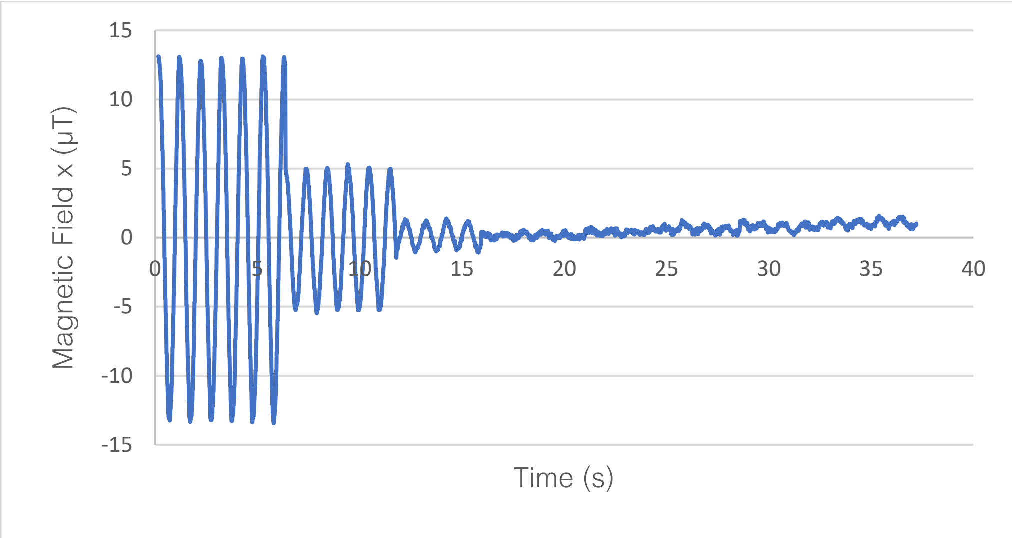

(a)

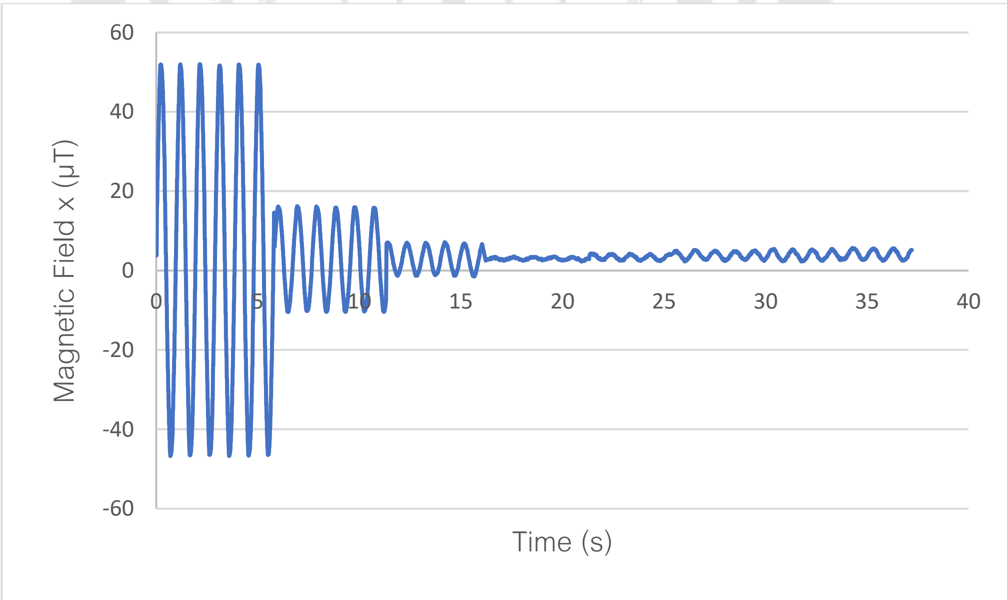

(b)

Figure 32 The relationship between magnetic field intensity and time for Case 3: (a) on the left side of the coil and (b) on the right side of the coil.

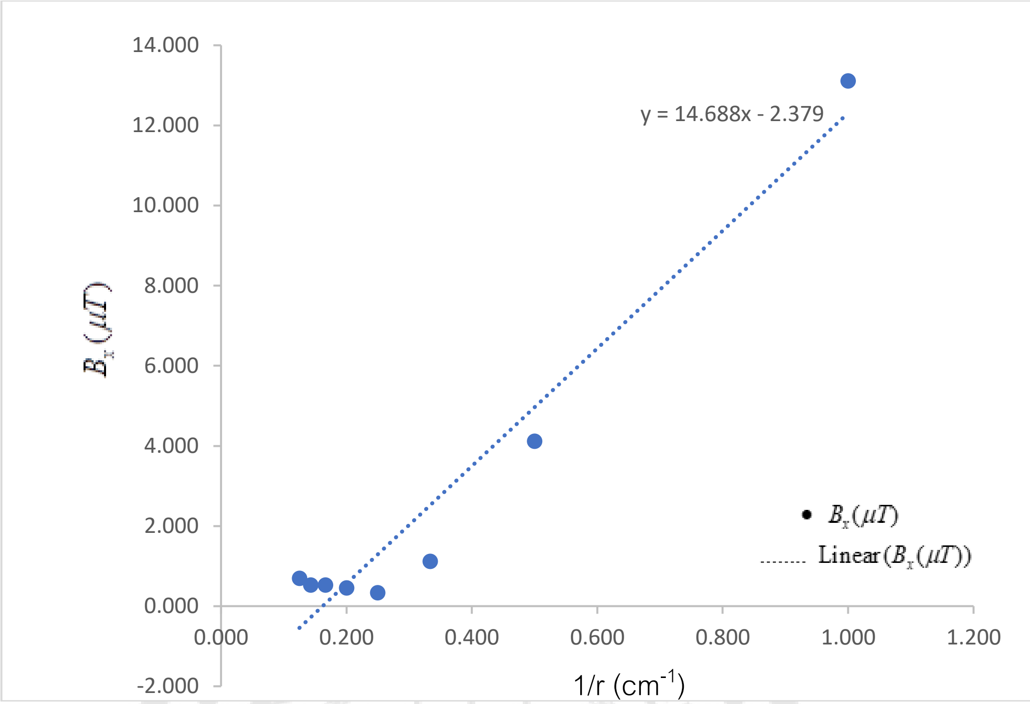

(a)

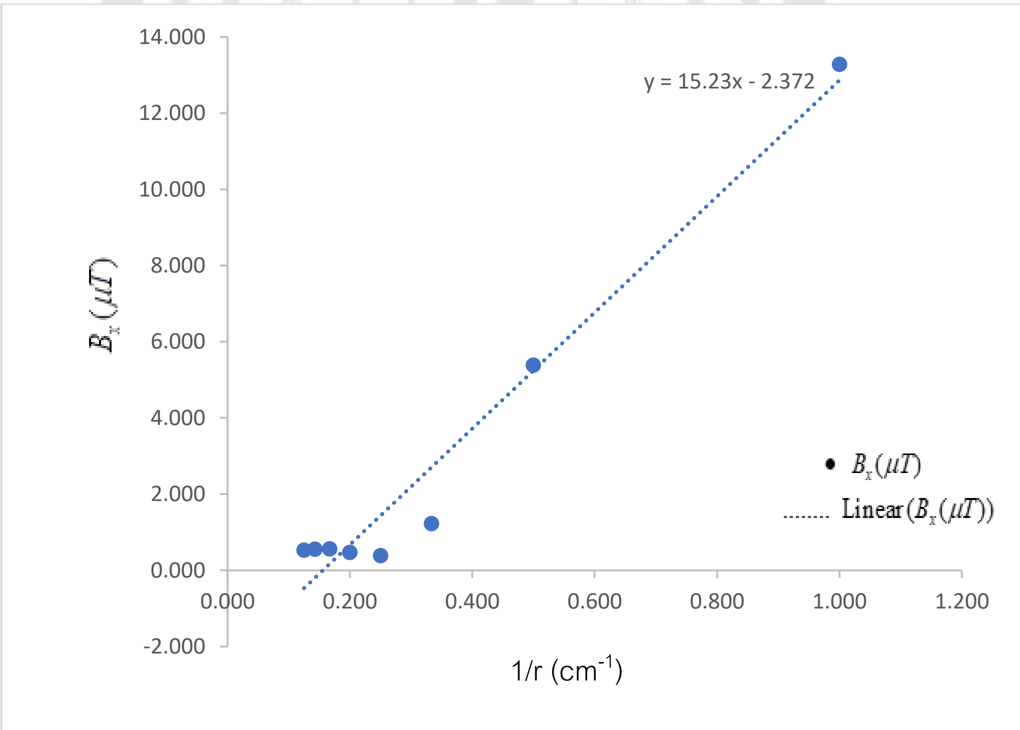

(b)

Figure 33 The relationship between the magnetic field intensity and the inverse of the distance from the coil for Case 3: (a) on the left side and (b) on the right side.

Table 4 The magnetic field intensity for Case 3 on the left sides and right sides of the coil.

$r\ (cm)$	$\frac{1}{r}\left(cm^{-1}\right)$	$B_{x(Left)}\left(\mu T\right)$	$B_{x(Right)}\left(\mu T\right)$
1	1.000	13.11	13.28
2	0.500	4.117	5.390
3	0.333	1.114	1.233
4	0.250	0.330	0.386
5	0.200	0.452	0.477
6	0.167	0.530	0.565
7	0.143	0.528	0.557
8	0.125	0.695	0.531

From the relationship graph in Figure 33, parts (a) and (b), the slopes were found to be $14.68\times10^{-8} T\cdot m$ and $15.23\times10^{-8} T\cdot m$, respectively. The calculated magnetic permeability of vacuum $\left(\mu_{Calculate}\right)$ were $1.188\times10^{-6} N\cdot A^{-2}$ and $1.233\times10^{-6} N\cdot A^{-2}$, with percent errors of 6.121% and 1.667%, respectively, when compared to the standard value.

4.1.4 Case 4: Two resistors in parallel

We set up an AC circuit with two 5-ohm, 20-watt resistors connected in parallel. The measured root means square current $\left(I_{rms}\right)$ was 2.130 A. Then, we calculated the peak current using the formula $I_{peak}=\sqrt{2}\,I_{rms}$, resulting in a peak current $\left(I_{peak}\right)$ of 3.000 A. Based on the data obtained from the magnetometer, we used Microsoft Excel 365 to display the relationship between magnetic field intensity and time, as shown in Figure 34. In this figure, (a) represents the magnetic field intensity on the left side of the coil, and (b) represents the intensity on the right side. We applied the equation $B_x=\left(\frac{B_{\max}-B_{\min}}{2}\right)$ to calculate the magnetic field intensity along the x-axis at distances from 1 cm to 8 cm from the coil. The results are presented in tables, with Table 5 showing the magnetic field intensity on the left and right sides of the coil.

Additionally, Figure 35 illustrates the relationship between the magnetic field intensity along the x-axis (B_x) and the inverse of the distance from the coil $\left(\frac{1}{r}\right)$, where (a) shows the intensity on the left side of the coil, and (b) shows the intensity on the right side.

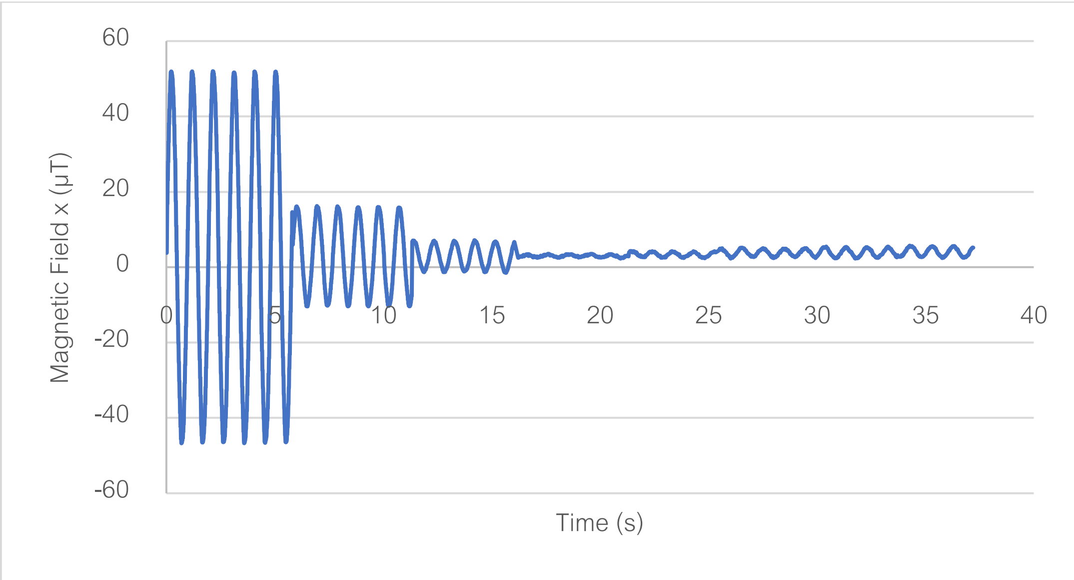

(a)

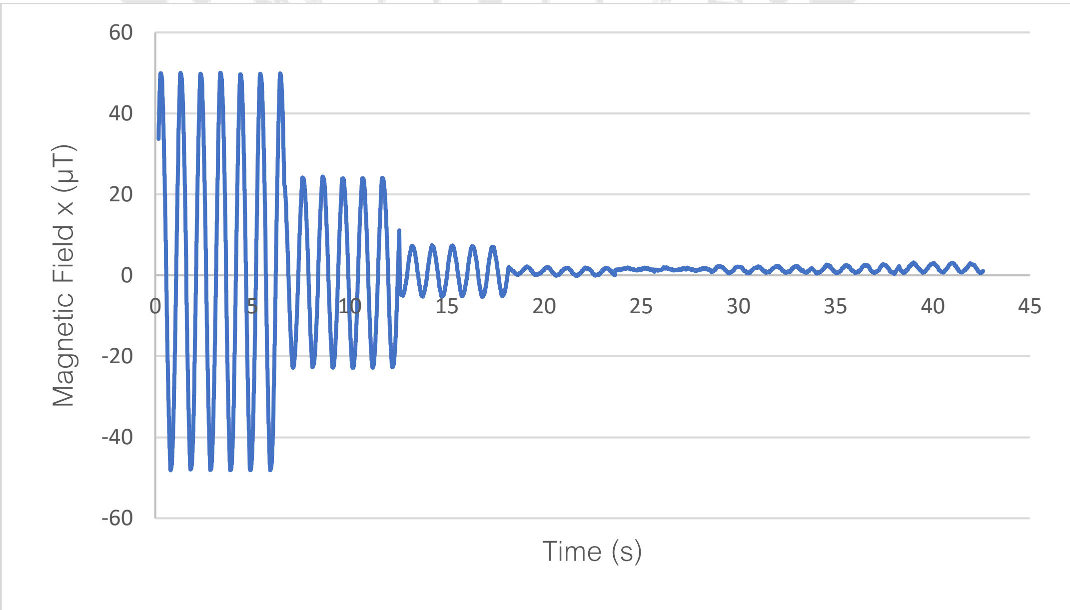

(b)

Figure 34 The relationship between magnetic field intensity and time for Case 4: (a) on the left side of the coil and (b) on the right side of the coil.

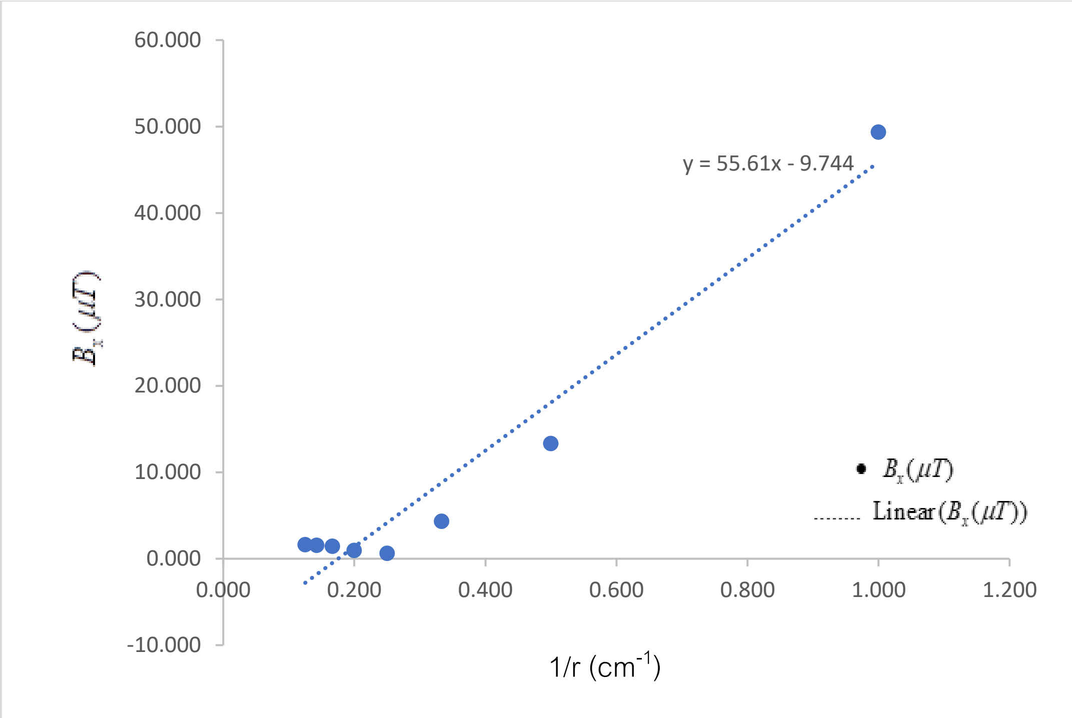

(a)

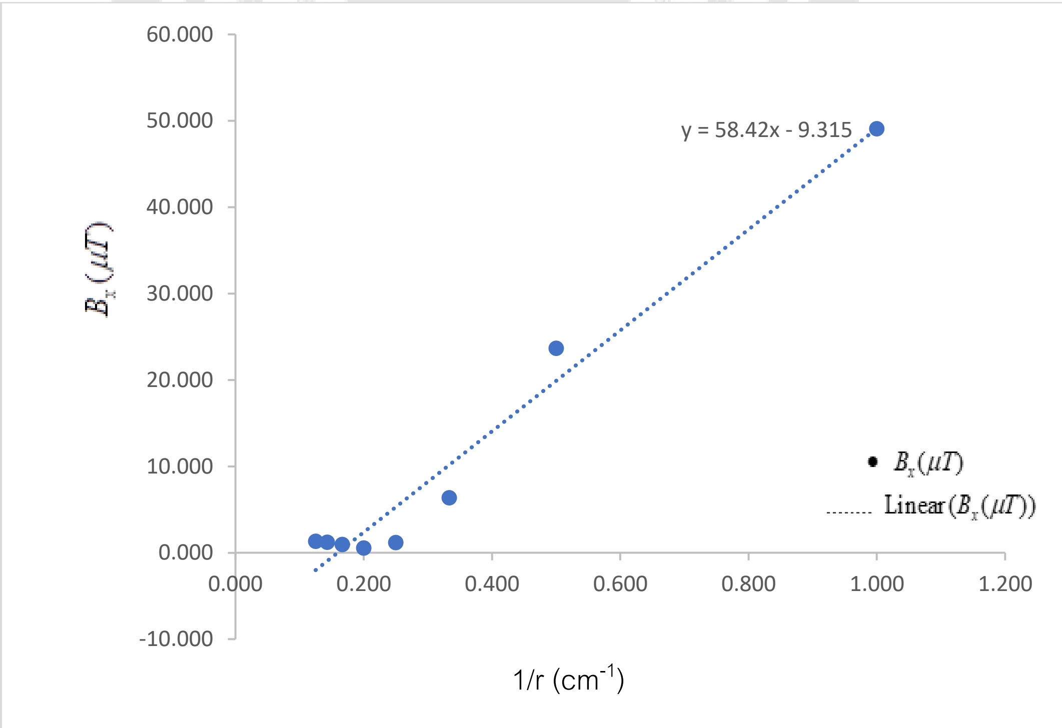

(b)

Figure 35 The relationship between the magnetic field intensity and the inverse of the distance from the coil for Case 4: (a) on the left side and (b) on the right side.

Table 5 The magnetic field intensity for Case 4 on the left and right sides of the coil.

$r\ (cm)$	$\frac{1}{r}\left(cm^{-1}\right)$	$B_{x(Left)}\left(\mu T\right)$	$B_{x(Right)}\left(\mu T\right)$
1	1.000	49.35	49.077
2	0.500	13.31	23.656
3	0.333	4.322	6.362
4	0.250	0.627	1.156
5	0.200	0.952	0.550
6	0.167	1.433	0.934
7	0.143	1.570	1.202
8	0.125	1.632	1.320

From the relationship graph in Figure 35, parts (a) and (b), the slopes were found to be $55.61\times10^{-8}T\cdot m$ and $58.42\times10^{-8}T\cdot m$, respectively. The calculated magnetic permeability of vacuum $\left(\mu_{Calculate}\right)$ were $1.162\times10^{-6}N\cdot A^{-2}$ and $1.221\times10^{-6}N\cdot A^{-2}$, with percent errors of 8.738% and 2.841%, respectively, when compared to the standard value.

4.1.5 Case 5: Three resistors in parallel

We set up an AC circuit with three 5-ohm, 20-watt resistors connected in parallel. The measured root means square current $\left(I_{rms}\right)$ was 2.613 A. Then, we calculated the peak current using the formula $I_{peak}=\sqrt{2}\,I_{rms}$, resulting in a peak current $\left(I_{peak}\right)$ of 3.698 A. Based on the data obtained from the magnetometer, we used Microsoft Excel 365 to display the relationship between magnetic field intensity and time, as shown in Figure 36. In this figure, (a) represents the magnetic field intensity on the left side of the coil, and (b) represents the intensity on the right side. We applied the equation $B_x=\left(\frac{B_{\max}-B_{\min}}{2}\right)$ to calculate the magnetic field intensity along the x-axis at distances from 1 cm to 8 cm from the coil. The results are presented in tables, with Table 6 showing the magnetic field intensity on the left and right sides of the coil. Additionally, Figure 37 illustrates the relationship between the magnetic field intensity along the x-axis (B_x) and the inverse of the distance from the coil $\left(\frac{1}{r}\right)$, where (a) shows the intensity on the left side of the coil, and (b) shows the intensity on the right side.

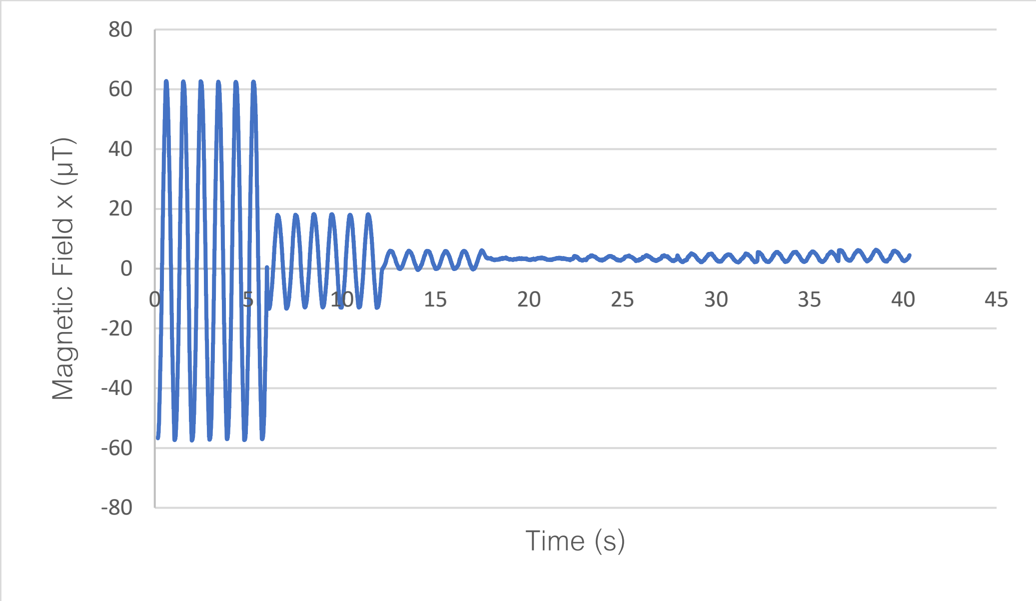

(a)

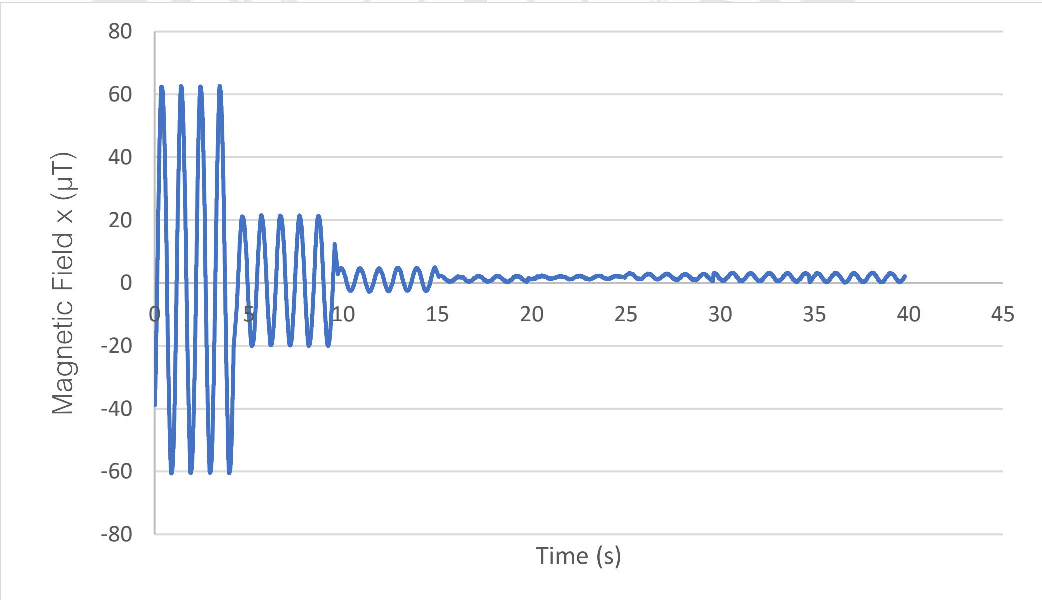

(b)

Figure 36 The relationship between magnetic field intensity and time for Case 5: (a) on the left side of the coil and (b) on the right side of the coil.

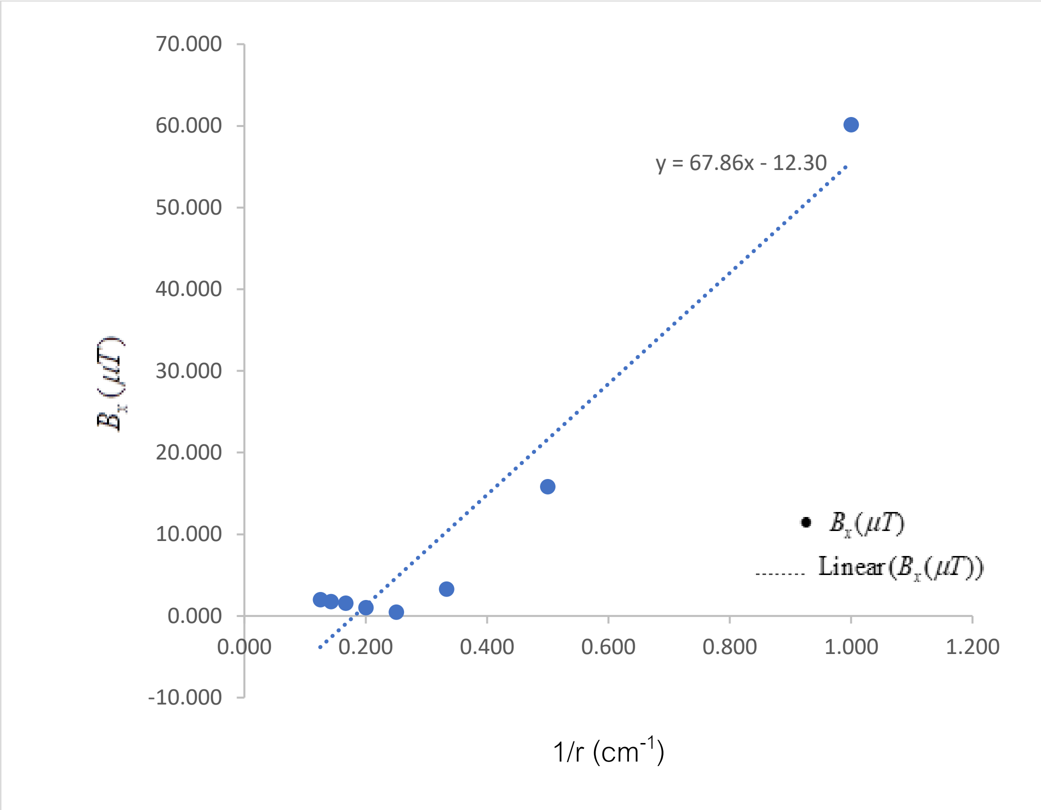

(a)

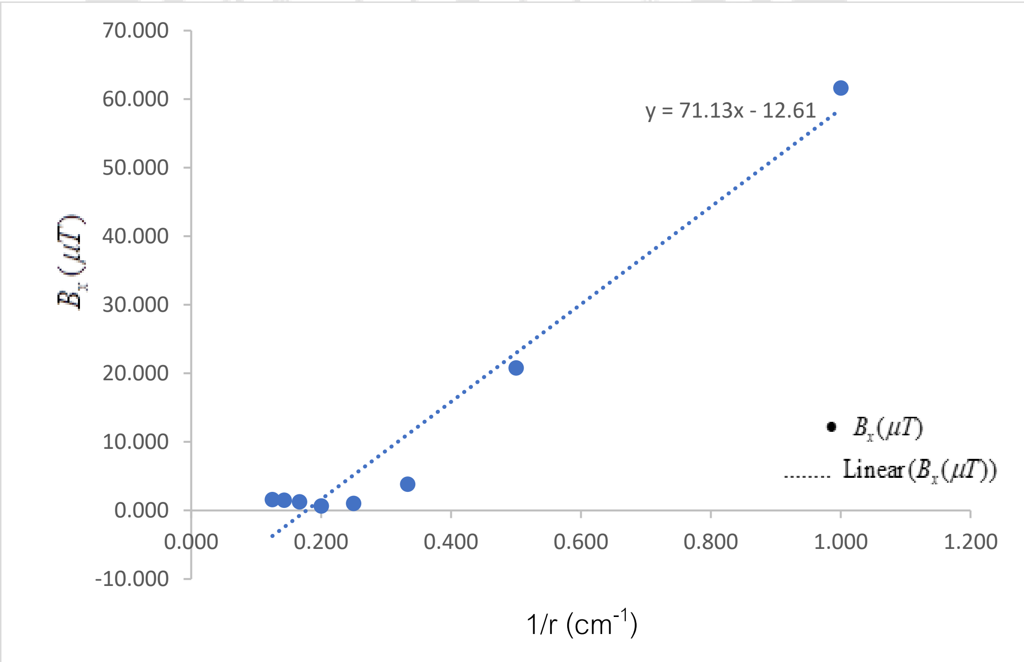

(b)

Figure 37 The relationship between the magnetic field intensity and the inverse of the distance from the coil for Case 5: (a) on the left side and (b) on the right side.

Table 6 The magnetic field intensity for Case 5 on the left and right sides of the coil.

$r\ (cm)$	$\frac{1}{r}\left(cm^{-1}\right)$	$B_{x(Left)}\left(\mu T\right)$	$B_{x(Right)}\left(\mu T\right)$
1	1.000	60.13	61.65
2	0.500	15.82	20.80
3	0.333	3.285	3.869
4	0.250	0.462	1.032
5	0.200	1.007	0.668
6	0.167	1.541	1.282
7	0.143	1.770	1.498
8	0.125	1.977	1.592

From the relationship graph in Figure 37, parts (a) and (b), the slopes were found to be $67.86\times10^{-8}T\cdot m$ and $71.13\times10^{-8}T\cdot m$, respectively. The calculated magnetic permeability of vacuum $\left(\mu_{Calculate}\right)$ were $1.156\times10^{-6}N\cdot A^{-2}$ and $1.207\times10^{-6}N\cdot A^{-2}$, with percent errors of 9.331% and 4.219%, respectively, when compared to the standard value.

From the experiment, the maximum electric current, permeability, and percent error of the permeability compared to the standard value were calculated. A summary of each case is presented in Table 7.

Table 7 The magnetic permeability from our experiment results.

I_{peak}(A)		slope ($T\cdot m$)	μ_c ($N\cdot A^{-2}$)	Error (%)
0.775	Left	14.68×10^{-8}	1.188×10^{-6}	6.121
	Right	15.23×10^{-8}	1.233×10^{-6}	1.667
1.128	Left	21.70×10^{-8}	1.208×10^{-6}	4.187
	Right	20.91×10^{-8}	1.164×10^{-6}	8.586
1.974	Left	36.26×10^{-8}	1.153×10^{-6}	9.643
	Right	36.79×10^{-8}	1.170×10^{-6}	7.957

Table 7 (Next) The magnetic permeability from our experiment results.

I_{peak} (A)	slope ($T \cdot m$)		μ_c ($N \cdot A^{-2}$)	Error (%)
3.000	Left	55.61×10^{-8}	1.162×10^{-6}	8.738
	Right	58.42×10^{-8}	1.221×10^{-6}	2.841
3.698	Left	67.86×10^{-8}	1.156×10^{-6}	9.330
	Right	71.13×10^{-8}	1.207×10^{-6}	4.219

4.2 Measuring the AC current in electrical appliances

Positioning the smartphone perpendicular to the north-south direction, at distances of 1 and 2 centimeters from the wire. Record the highest and lowest magnetic field values, then calculate the magnetic field of the electrical appliance as half the difference between these values $B_x = \left(\frac{B_{\max} - B_{\min}}{2}\right)$. The linear relationship between the magnetic field and electric current was measured and is shown in Figure 38. In this case, the solid and dashed lines correspond to the equations $B(\mu T) = 29.93I(A) - 2.572$ and $B(\mu T) = 4.950I(A) + 0.581$, representing distances of 1 cm and 2 cm from the wire, respectively. For practical applications, we rearranged these equations to $I(A) = (B(\mu T) + 2.572)/29.93$ and $I(A) = (B(\mu T) - 0.581)/4.953$ for the 1 cm and 2 cm distances. We then tested these equations to measure the current of three different types of electrical equipment, using a clamp meter, a multimeter, and a smartphone for comparison. The results are presented in Table 8.

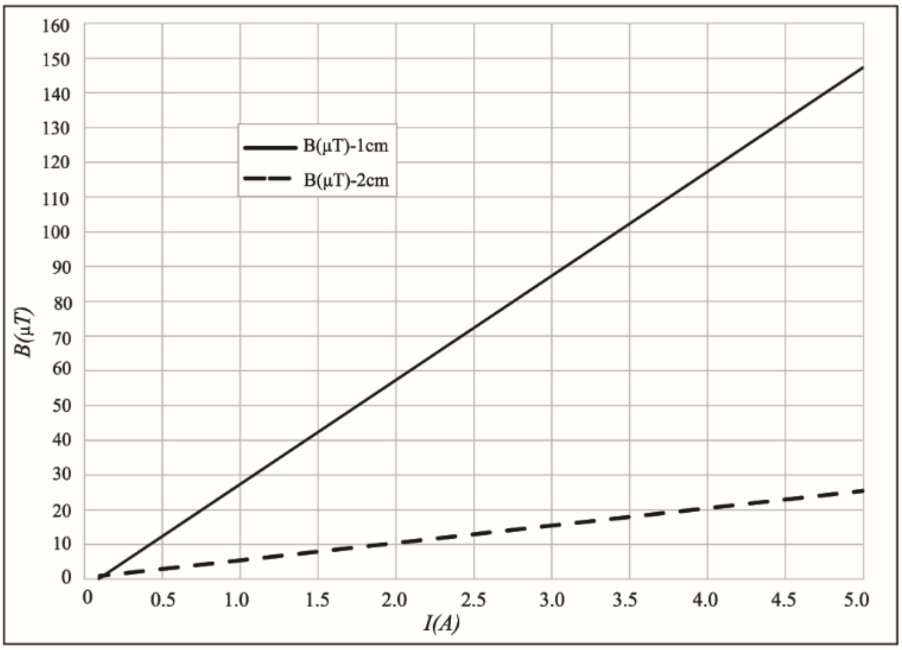

Figure 38 The relationship between the magnetic field and AC current.

Table 8 Compares the average current to the multimeter and clamp meter readings.

Electrical appliance	1 cm		2 cm		I av (A)	I (A) Multimeter	I (A) Clamp	% meter	% Clamp
	B(μT)	I (A)	B (μT)	I (A)					
1	7.959	0.350	2.428	0.370	0.370	0.391	0.392	5.370	5.610
	8.020	0.350	2.731	0.430					
	8.168	0.360	2.270	0.340					
2	25.60	0.940	6.536	1.200	1.090	1.030	1.070	5.830	1.870
	25.68	0.940	7.000	1.300					
	22.88	0.850	7.181	1.330					
3	30.75	1.110	9.569	1.810	1.390	1.410	1.450	1.420	4.130
	36.31	1.300	7.849	1.470					
	33.18	1.190	7.880	1.470					

Table 8 (Next) Compares the average current to the multimeter and clamp meter readings.

Electrical appliance	1 cm		2 cm		I av (A)	I (A) Multimeter	I (A) Clamp	% meter	% Clamp
	B (μT)	I (A)	B (μT)	I (A)					
4	38.66	1.380	10.58	2.020	1.730	1.660	1.700	4.210	1.760
	39.65	1.410	10.77	2.060					
	39.19	1.390	10.97	2.100					

CHAPTER 5
CONCLUSIONS

The research on developing a demonstration laboratory kit for measuring the magnetic field using a smartphone application, specifically for a straight electrical wire, aimed to create a kit to study magnetic fields based on Ampere's Law and to test its effectiveness. The study was divided into two main parts: measuring the magnetic field produced by current in a single straight wire and measuring the AC current in electrical appliances.

In the first part, we measured the magnetic field at eight points to the left and eight points to the right of the wire, with each point spaced 1 cm apart. The circuit consisted of five configurations using a 5-ohm, 20-watt resistor: a single resistor (Case 1), two resistors in series (Case 2), three resistors in series (Case 3), two resistors in parallel (Case 4), and three resistors in parallel (Case 5). Magnetic field measurements were taken at distances from 1 cm to 8 cm from the straight wire on both sides for each case, recording the highest and lowest magnetic field values. The magnetic field of electrical equipment was calculated as half the difference between these values, and the root mean square current (I_{rms}) was determined. From this, the peak current (I_{peak}) was calculated, ranging from 0.775 A to 3.698 A across all five cases. When analyzing the relationship between magnetic field intensity and the inverse of the distance from the wire for all five cases, the slope varied, starting at $14.68\times10^{-8} T\cdot m$ and increasing to $71.13\times10^{-8} T\cdot m$. Ampere's Law was then used to calculate magnetic permeability, which ranged from $1.156\times10^{-6} N\cdot A^{-2}$ to $1.233\times10^{-6} N\cdot A^{-2}$. Compared to the standard magnetic permeability $\left(1.256\times10^{-6} N\cdot A^{-2}\right)$, the percentage errors ranged between 1.667% and 9.643%. Magnetic permeability is essential for calculating and explaining the behavior of magnetic fields in various systems. The magnetic permeability calculations in this research demonstrated consistent accuracy, with deviations within 10% of standard values, which were considered highly satisfactory.

In the second part, we measured the magnetic field in a circuit connected to an electrical appliance using four configurations. Measurements were taken at distances of

1 cm and 2 cm for each configuration, yielding the highest and lowest magnetic field values. The magnetic field of the electrical appliance was then calculated as half the difference between these values. When analyzing the relationship between magnetic field intensity and electrical current, it was found that all four configurations had an average current starting at 0.370 A and increasing to 1.730 A. The multimeter readings ranged from 0.391 A to 1.660 A, while the clamp meter readings ranged from 0.392 A to 1.700 A. When comparing the calculated current values with those measured using multimeter, the percentage errors were between 1.420% and 5.830%. Similarly, compared with the clamp meter, the percentage errors ranged from 1.760% to 5.610%. These deviations, all within 5.830%, indicate satisfactory consistency and accuracy.

Therefore, the demonstration kit for studying magnetic fields based on Ampere's Law developed in this research is effective enough to serve as a prototype for laboratory experiments in general physics at both the high school and university levels. Additionally, it can be used in future research projects for tryouts with students to enhance their learning outcomes in physics.

REFERENCES

Arabasi, S., & Al-taani, H. (2016). Measuring the Earth's magnetic field dip angle using a smartphone-aided setup: a simple experiment for introductory physics laboratories. *European Journal of Physics, 38*(2), 025201.

Arribas, E., Escobar, I., Ramirez-Vazquez, R., del Pilar Suarez Rodriguez, C., Gonzalez-Rubio, J., & Belendez, A. (2020). Linear quadrupole magnetic field measured with a smartphone. *The Physics Teacher, 58*(3), 182-185.

Carroll, R., & Lincoln, J. (2020). Phyphox app in the physics classroom. *The Physics Teacher, 58*(8), 606-607.

Chamonwang, S., & Chanunun, S. (2023). Developing the ability to communicate science by organizing learning using phenomena as a basis together with visual thinking strategies about substances in daily life of fifth grade primary school students . *Journal of Roi Kaensarn Academi, 8*(10), 119-136.

Cucos, C., & Iucu, R. (2020). Management of continuous training programs for teachers. Practical guide. *Educatia 21*(19), 193-196.

Daggol, G. (2017). Lifelong learning: Not a 21st century, but an omnitemporal skill. *International Journal of Social and Humanities Sciences Research (JSHSR), 4*(12), 1254-1267.

Drory, A. (2023). Motivating the Biot-Savart Law. *The Physics Teacher, 61*(5), 368-368.

Dwyer, R. J., Kushlev, K., & Dunn, E. W. (2018). Smartphone use undermines enjoyment of face-to-face social interactions. *Journal of Experimental Social Psychology, 78*, 233-239.

Enrique, A., Escobar, I., Suarez, C. P., Najera, A., & Beléndez, A. (2015). Measurement of the magnetic field of small magnets with a smartphone: a very economical laboratory practice for introductory physics courses. *European Journal of Physics, 36*(6), 065002.

Galili, I. (2018). Physics and mathematics as interwoven disciplines in science education. *Science & Education, 27*(1-2), 7-37.

Griffiths, D. J. (2023). *Introduction to electrodynamics*. The United Kingdom: Cambridge University Press.

Guo, J., & Woulfin, S. (2016). Twenty-first century creativity: An investigation of how the partnership for 21st century instructional framework reflects the principles of creativity. *Roeper Review, 38*(3), 153-161.

Habermas, J. (2015). *Knowledge and human interests*. United state of America: John Wiley & Sons.

Halliday, D., Resnick, R., & Jearl, W. (2007). *Fundaments of physics*. The United States of America: Cleveland state University.

Khvorostianov, N. (2023). Smartphone use by Ukrainian refugee children. *new media & society*, 14614448231173657.

Likkason, O. K. (2014). Exploring and using the magnetic methods. *Advanced geoscience remote sensing. InTech, Croatia*, 141-174.

Ling, S. J., Moebs, W., & Sanny, J. (2016). Physics *University Physics Volume 2*.

Matarboumosleh, J., & Jaalouk, D. (2017). Depression, anxiety, and smartphone addiction in university students-A cross sectional study. *PloS one, 12*(8), e0182239.

Nazar, A. M., Jiao, P., Zhang, Q., Egbe, K.-J. I., & Alavi, A. H. (2021). A new structural health monitoring approach based on smartphone measurements of magnetic field intensity. *IEEE Instrumentation & Measurement Magazine, 24*(4), 49-58.

Pathak, P., & Patel, Y. (2022). Analyzing a Free-Falling Magnet to Measure Gravitational Acceleration Using a Smartphone's Magnetometer. *The Physics Teacher, 60*(6), 441-443.

Pierratos, T., & Polatoglou, H. M. (2020). Utilizing the phyphox app for measuring kinematics variables with a smartphone. *Physics education, 55*(2), 025019.

Pili, U., & Violanda, R. (2018). Measuring average angular velocity with a smartphone magnetic field sensor. *The Physics Teacher, 56*(2), 114-115.

Ramaneeya, S. (2016). Results of using an application for teaching English vocabulary on tablets in the subject of English for 2nd year primary school students under the Ratchaburi Primary Educational Service Area Office 2;. *Veridian E-Journal,* *Silpakorn University (Humanities, Social Sciences and arts), 9*(2), 1030-1045.

Salvatore, P., Enrico, P., Daniela, Z., & Melda, K. (2019). Multimethodological approach to investigate urban and suburban archaeological sites. In *Innovation in Near Surface Geophysics* (pp. 461-504).

Samimi, M. H., Tenbohlen, S., Akmal, A. A. S., & Mohseni, H. (2016). Effect of different connection schemes, terminating resistors and measurement impedances on the sensitivity of the FRA method. *IEEE Transactions on Power Delivery, 32*(4), 1713-1720.

Setiawan, B., Septianto, R., Suhendra, D., & Iskandar, F. (2017). Measurement of 3-axis magnetic fields induced by current wires using a smartphone in magnetostatics experiments. *Physics education, 52*(6), 065011.

Staacks, S., Dorsel, D., Hütz, S., Stallmach, F., Splith, T., Heinke, H., & Stampfer, C. (2022). Collaborative smartphone experiments for large audiences with phyphox. *European Journal of Physics, 43*(5), 055702.

Tanawesh, k. (2014). Developing scientific concepts on magnetic and electric field using simple experiment and multimedia learning. *Ubon Ratchathani University Portal site for E-Thesis & E-Research*.

Teh, H. Y., Kempa Liehr, A. W., & Wang, K. I. K. (2020). Sensor data quality: A systematic review. *Journal of Big Data, 7*(1), 11.

Thipwan, M., Somprasong, P., Nattiphon, C., Rattanasuda, S., & Thanaphong, C. (2021). Creating a simple alternating current magnetic field measuring device for teaching . *Journal of Science & Technology MSU, 40*(2).

Torbert, R. B., Burch, J., Giles, B., Gershman, D., Pollock, C., Dorelli, J., . . . Strangeway, R. J. (2016). Estimates of terms in Ohm's law during an encounter with an electron diffusion region. *Geophysical Research Letters, 43*(12), 5918-5925.

Wannous, J., & Horvath, P. (2023). Precise Measurements Using a Smartphone’s Magnetometer Measuring Magnetic Fields and Permeability. *The Physics Teacher, 61*(1), 36-39.

Westermann, N., Staacks, S., Heinke, H., & Möhrke, P. (2022). Measuring the magnetic field of a low frequency LC-circuit with phyphox. *Physics education, 57*(6), 065024.

Williams, J. E. (2014). Measuring Earth's local magnetic field using a Helmholtz coil. *The Physics Teacher, 52*(4), 236-238.

Yang, D., Liu, W., & Wu, X. (2023). Impact of electric charges on chaos in magnetized reissner nordström spacetimes. *The European Physical Journal C, 83*(5), 357.

Zangwill, A. (2013). *Modern electrodynamics*. The United Kingdom: Cambridge University Press.

Zhao, Y., Li, X. g., Zhou, X., & Zhang, Y. n. (2016). Review on the graphene based optical fiber chemical and biological sensors. *Sensors and Actuators B: Chemical, 231*, 324-340.

VITA

NAME	Mr. Pathom Vongvizay
DATE OF BIRTH	05 April 1993
PLACE OF BIRTH	Hadchaiphong village, Nongbok District, Khammuance Province, Lao PDR.
INSTITUTIONS ATTENDED	2005 Secondary School from Tanteng Secondary School, Nongbok District, Khammuance Province 2011 High School from Navang High School, Nongbok District, Khammuance Province 2015 Graduated in Physics from National University of Laos.
HOME ADDRESS	Hadchaiphong village, Nongbok District, Khammuance province, Lao PDR.